msp

Algebraic & Geometric Topology 17 (2017) 2239–2282

The diagonal slice of Schottky space

CAROLINE SERIES
SER PEOW TAN
YASUSHI YAMASHITA

An irreducible representation of the free group on two generators X, Y into $\mathrm{SL}(2,\mathbb{C})$ is determined up to conjugation by the traces of X, Y and XY. If the representation is faithful and discrete, the resulting manifold is in general a genus-2 handlebody. We study the diagonal slice of the representation variety in which $\mathrm{Tr}\, X = \mathrm{Tr}\, Y = \mathrm{Tr}\, XY$. Using the symmetry, we are able to compute the Keen–Series pleating rays and thus fully determine the locus of faithful discrete representations. We also computationally determine the "Bowditch set" consisting of those parameter values for which no primitive elements in $\langle X, Y\rangle$ have traces in $[-2, 2]$, and at most finitely many primitive elements have traces with absolute value at most 2. The graphics make clear that this set is both strictly larger than, and significantly different from, the discreteness locus.

30F40; 57M50

1 Introduction

It is well known that an irreducible representation ρ of the free group F_2 on two generators X, Y into $\mathrm{SL}(2,\mathbb{C})$ is determined up to conjugation by the traces of $\rho(X)$, $\rho(Y)$ and $\rho(XY)$. More generally, if we take the GIT quotient of all (not necessarily irreducible) representations, then the resulting $\mathrm{SL}(2,\mathbb{C})$ character variety of F_2 can be identified with $\mathbb{C}^3$ via these traces using an old result of Vogt; see for example Goldman [10]. If the representation is faithful, discrete, purely loxodromic and geometrically finite, the resulting manifold is a genus-2 handlebody; see Section 3. The collection of all such representations is known as *Schottky space*, denoted by $\mathcal{SCH}$. It is a consequence of Bers' density theorem that $\mathcal{SCH}$ is the interior of the faithful discreteness locus; see for example Canary [4]. It is natural to ask: for which values of $x = \mathrm{Tr}\,\rho(X)$, $y = \mathrm{Tr}\,\rho(Y)$, $z = \mathrm{Tr}\,\rho(XY)$ is the corresponding representation in $\mathcal{SCH}$?

Let $\mathcal{P}$ denote the set of primitive elements of F_2 modulo conjugation and inverse. For $(x, y, z) \in \mathbb{C}^3$, let $\rho_{(x,y,z)}$ denote a choice of representation $F_2 \to \mathrm{SL}(2,\mathbb{C})$ in the conjugacy class determined by the trace triple. The *Bowditch set* (or BQ–set) $\mathcal{B}$ is

Published: 3 August 2017 DOI: 10.2140/agt.2017.17.2239

defined in Tan, Wong and Zhang [30] as the set of $(x, y, z) \in \mathbb{C}^3$ corresponding to irreducible representations for which

$$\operatorname{Tr}\rho_{(x,y,z)}(g) \notin [-2, 2] \text{ for all } g \in \mathcal{P} \quad \text{and} \quad \{g \in \mathcal{P} : |\operatorname{Tr}\rho_{(x,y,z)}(g)| \leq 2\} \text{ is finite.}$$

(The exceptional case in which $\operatorname{Tr}\rho([X, Y]) = 2$ corresponds to reducible representations and is excluded from the discussion; see Remark 2.1.) The Bowditch set is open, and the set of outer automorphisms $\mathrm{Out}(F_2)$ of F_2 acts properly discontinuously on it. Thus it is essentially the domain of discontinuity for the mapping class group acting on traces of primitive words. Clearly, $\mathcal{SCH} \subset \mathcal{B}$.

Bowditch's original work [3] was on the case in which the image of the commutator $[X, Y] = XYX^{-1}Y^{-1}$ is parabolic and $\operatorname{Tr}\rho([X, Y]) = -2$. He conjectured that the subsets of $\mathcal{SCH}$ and $\mathcal{B}$ corresponding to this restriction coincide. Although this has not been proven, computer pictures indicate his conjecture may well be true.

In this paper, we restrict to the special case in which $x = y = z$, which we call the *diagonal slice* of the character variety, denoted by Δ and parametrised by the single complex variable x. We show that in this slice, the analogue of Bowditch's conjecture is far from being true. This is illustrated in Figure 1, which compares the intersections of Δ with $\mathcal{SCH}$ and $\mathcal{B}$. The discreteness locus is the outer region foliated by rays; these are the Keen–Series pleating rays which relate to the geometry of the convex hull boundary as explained in Section 4.2 and whose closure is known to be $\overline{\Delta \cap \mathcal{SCH}}$; see Theorem 4.23. The Bowditch set, by contrast, is the complement of the black part. It is clear that $\mathcal{B} \cap \Delta$ contains a large open region not in $\Delta \cap \mathcal{SCH}$, and also has different symmetries. In particular, it is not hard to show that the interval $(2, 3)$ is contained in $\mathcal{B} \setminus \mathcal{SCH}$; see the discussion in Section 2.2.2.

We would like to emphasise that there are two problems at issue here; namely, to find the locus of discrete faithful representations, and to find the domain of discontinuity for the automorphism group $\mathrm{Out}(F_2)$ acting on traces of primitive words. Both of these problems are quite difficult and subtle with not many previous results. Moreover, while there appeared to be some evidence from earlier studies that the two sets might, modulo some minor caveats, coincide, our results indicate that on the contrary they are unlikely to be related, or at least that their relationship is not obvious.

The main content of this paper is an explanation and justification of how these plots were made, in particular, to explain how we enumerated and computed the pleating rays for the symmetric genus-2 handlebody corresponding to the trace triple (x, x, x).

To compute the Bowditch set $\mathcal{B}$ we use an algorithm based on the ideas in [3] and developed further in [30]. This is explained in Section 2.2.1.

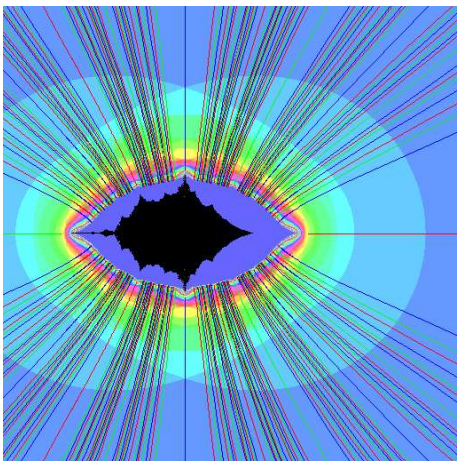

Figure 1: Superposition of the discreteness locus for $\pi_1(\mathcal{H})$ and the Bowditch set in the x–plane. The Bowditch set for the (x,x,x)–triple is the complement of the central black region, while the discreteness locus is the closure of the region foliated by rays. The rays are actually computed as the pleating rays for the quotient orbifold $\mathcal{S}$. The vertical ray is at $x=\frac{1}{2}$, and the discreteness locus intersects $\mathbb{R}$ in $(-\infty,-2]$ and $[3,\infty)$; see Section 4.5.

The discreteness problem is tackled as follows. If $(x,x,x)\in\mathcal{SCH}$, then the quotient 3–manifold $\mathbb{H}^3/G$ is a handlebody $\mathcal{H}$ with order-3 symmetry. We use the symmetry to reduce the problem of finding $\Delta\cap\mathcal{SCH}$ to a problem very similar to that of determining the so-called *Riley slice of Schottky space*. This is actually a space of groups on the boundary of $\mathcal{SCH}$, consisting of those free, discrete and geometrically finite groups for which the two generators $\rho(X)$, $\rho(Y)$ are parabolic, thus contained in the slice $(2,2,z)\subset\mathbb{C}^3$. The corresponding manifold is a handlebody whose conformal boundary is a sphere with four parabolic points. The problem of finding those z–values for which such a group is free, discrete and geometrically finite was solved using the method of pleating rays in Keen and Series [15]. In the present case, the quotient of $\mathcal{H}$ by the symmetry is an orbifold $\mathcal{S}$ with two order-3 cone axes, whose conformal boundary is a sphere with four order-3 cone points. Thus similar methods enable us to find $\Delta\cap\mathcal{SCH}$ here.

Although Figure 1 shows that in Δ, the analogue of Bowditch's conjecture fails since $\mathcal{B}$ and the interior of the discreteness locus are plainly distinct, in many other slices (see for example Figure 8), the (modified) Bowditch set and the interior of the discreteness locus appear to coincide. This is connected to the dynamics of the action of a suitable mapping class group on representations and raises many interesting questions which we hope to address elsewhere.

The plan of the paper is as follows. We begin in Section 2 with a discussion of the Markoff tree and the algorithm used to compute the Bowditch set. In Section 3, we introduce a basic geometrical construction which conveniently encapsulates the 3–fold symmetry. The quotient of the original handlebody $\mathcal{H}$ by the symmetry is a ball with two order-3 cone axes. This orbifold $\mathcal{S}$ has a further 4–fold symmetry group whose quotient is again a topological ball. Our construction allows us to write down specific $\mathrm{SL}(2,\mathbb{C})$ representations (in some cases, $\mathrm{PSL}(2,\mathbb{C})$ representations; see the discussion in Section 3.1 and in particular Remark 3.2) of all the groups involved with ease. In Section 4, we turn to the discreteness question. After reducing the problem to one on $\mathcal{S}$, we briefly review material from the Keen–Series theory of pleating rays and recall what is needed from [15], allowing us to apply a similar proof in the present context. Section 5, not strictly logically necessary for our development, explains how we did our trace computations in practice, by relating the problem to one on a commensurable torus with a single cone point of angle $\frac{4\pi}{3}$.

Acknowledgements We would like to thank the referee for a very careful reading of the paper which resulted in significant improvements.

Tan is partially supported by the National University of Singapore academic research grant R-146-000-186-112. Yamashita is partially supported by JSPS KAKENHI grant number 23540088.

2 The Markoff tree and the Bowditch set

Let $A = \left(\begin{smallmatrix} a & b \\ c & d \end{smallmatrix}\right) \in \mathrm{SL}(2,\mathbb{C})$ so that $ad - bc = 1$. As usual we define its trace $\operatorname{Tr} A = a + d$.

Let $F_2 = \langle X, Y \mid - \rangle$ be the free group on two generators. It is well known that a representation $\rho\colon F_2 \to \mathrm{SL}(2,\mathbb{C})$ is determined up to conjugation (modulo taking the GIT quotient under the conjugation action; see [10]) by the three traces $x = \operatorname{Tr}\rho(X)$, $y = \operatorname{Tr}\rho(Y)$, $z = \operatorname{Tr}\rho(XY)$. In fact, given $x, y, z \in \mathbb{C}$, we can define a representation

$$\rho_{x,y,z}\colon F_2 \to \mathrm{SL}(2,\mathbb{C}), \quad \rho(X) = \begin{pmatrix} x & 1 \\ -1 & 0 \end{pmatrix},\ \rho(Y) = \begin{pmatrix} 0 & \eta \\ -\eta^{-1} & y \end{pmatrix},$$

where $z = -(\eta + \eta^{-1})$; see [9]. Clearly, with this definition, $\operatorname{Tr}\rho(X) = x$, $\operatorname{Tr}\rho(Y) = y$ and $\operatorname{Tr}\rho(XY) = z$.

2.1 The Markoff tree

For matrices $\widehat{U}, \widehat{V} \in \mathrm{SL}(2,\mathbb{C})$, set $u = \operatorname{Tr}\widehat{U}$, $v = \operatorname{Tr}\widehat{V}$, $w = \operatorname{Tr}\widehat{U}\widehat{V}$ (where we use the notation $\widehat{U}, \widehat{V}$ to distinguish from generators U, V of F_2). Recall the trace

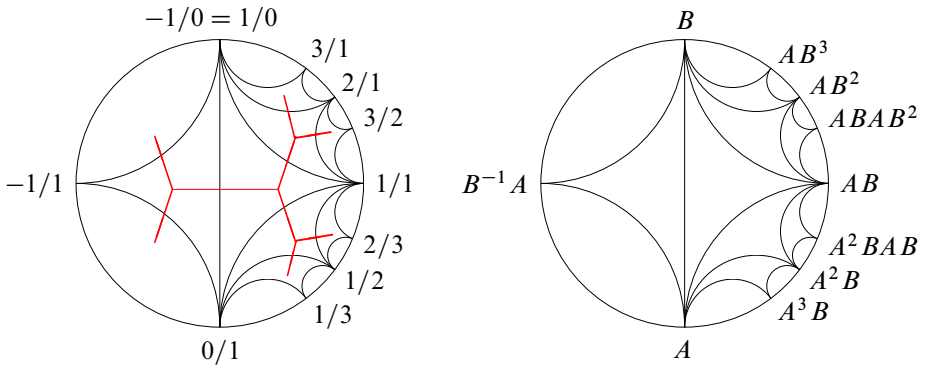

Figure 2: The Farey diagram, showing the arrangement of rational numbers on the left with the corresponding primitive words on the right

relations

$$\operatorname{Tr} \widehat{U}\,\widehat{V}^{-1} = uv - w, \tag{2-1}$$

$$u^2 + v^2 + w^2 = uvw + \operatorname{Tr}[\widehat{U}, \widehat{V}] + 2. \tag{2-2}$$

Setting $\mu = \operatorname{Tr}[\widehat{U}, \widehat{V}] + 2$, this last equation takes the form

$$u^2 + v^2 + w^2 - uvw = \mu.$$

Let $F_2 = \langle X, Y \mid - \rangle$ as above. An element $U \in F_2$ is *primitive* if it is a member of a generating pair; we denote the set of all primitive elements by $\mathcal{P}$. The conjugacy classes of primitive elements are enumerated by $\widehat{\mathbb{Q}} = \mathbb{Q} \cup \infty$ and are conveniently organised relative to the Farey diagram $\mathcal{F}$ as shown in Figure 2. This consists of the images of the ideal triangle with vertices at $1/0, 0/1$ and $1/1$ under the action of $\mathrm{SL}(2, \mathbb{Z})$ on the upper half plane, suitably conjugated to the position shown in the disk. The label p/q in the disk is just the conjugated image of the actual point $p/q \in \mathbb{R}$.

Since the rational points are precisely the images of ∞ under $\mathrm{SL}(2, \mathbb{Z})$, they correspond bijectively to the vertices of $\mathcal{F}$. A pair $p/q, r/s \in \widehat{\mathbb{Q}}$ are the endpoints of an edge if and only if $pr - qs = \pm 1$; such pairs are called *neighbours*. A triple of points in $\widehat{\mathbb{Q}}$ are the vertices of a triangle precisely when they are the images of the vertices of the initial triangle $(1/0, 0/1, 1/1)$; such triples are always of the form $(p/q, r/s, (p+r)/(q+s))$ where p/q, r/s are neighbours. In other words, if p/q, r/s are the endpoints of an edge, then the vertex of the triangle on the side away from the centre of the disk is found by "Farey addition" to be $(p + r)/(q + s)$. Starting from $1/0 = -1/0 = \infty$ and $0/1$, all points in $\widehat{\mathbb{Q}}$ are obtained recursively in this way. (Note we need to start with $-1/0 = \infty$ to get the negative fractions on the left side of the left-hand diagram in Figure 2.)

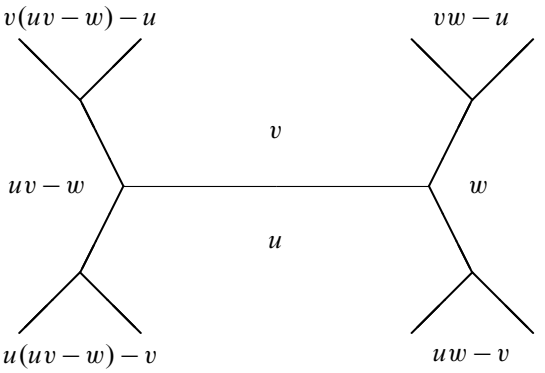

Figure 3: The Markoff tree used to compute traces with an initial triple (u, v, w)

The right-hand picture in Figure 2 shows a corresponding arrangement of primitive elements in F_2, one in each conjugacy class, starting with initial triple (A, B, AB). Each vertex is labelled by a certain cyclically reduced representative of the corresponding word. Pairs of primitive elements form a generating pair if and only if they are at the endpoints of an edge. Triples at the vertices of a triangle correspond to a generator triple of the form (U, V, UV). Corresponding to the process of Farey addition, successive words can be found by juxtaposition as indicated on the diagram. Note that for this to work, it is important to preserve the order: if U, V are the endpoints of an edge with U before V in the anticlockwise order round the circle, the correct concatenation is UV. Note also that the words on the left side of the diagram involve $B^{-1}A$, corresponding to starting with $\infty = -1/0$. We denote the particular representative of the conjugacy class corresponding to $p/q \in \hat{\mathbb{Q}}$ found by concatenation by $W_{p/q}$. Its word length in the generators A, B is a function $F(p/q)$ of p/q. A function on $\hat{\mathbb{Q}}$ is said to have *Fibonacci growth* if it is comparable with uniform upper and lower bounds to F.

In this paper, we are largely interested in computing traces of primitive elements. Following Bowditch [3], these can also be easily computed by using the trivalent tree $\mathbb{T}$ dual to $\mathcal{F}$; see the left frame of Figure 2 and Figure 3. Let Ω denote the set of complementary regions of $\mathbb{T}$; abstractly, a complementary region is the closure of a connected component of the complement of $\mathbb{T}$. As is apparent from Figure 2, there is a bijection between Ω and the set of vertices of $\mathcal{F}$. Thus the set Ω can be identified with conjugacy classes of primitive elements and hence with $\hat{\mathbb{Q}}$.

Given a representation $\rho\colon F_2 \to \mathrm{SL}(2,\mathbb{C})$, each $U \in \Omega$ is labelled by $u = \operatorname{Tr}\rho(U)$, the trace of the corresponding generator, as shown in Figure 3. Labels on opposite sides of an edge of $\mathbb{T}$ correspond to traces of a generator pair: the three labels round a vertex correspond to a generator triple (U, V, UV).

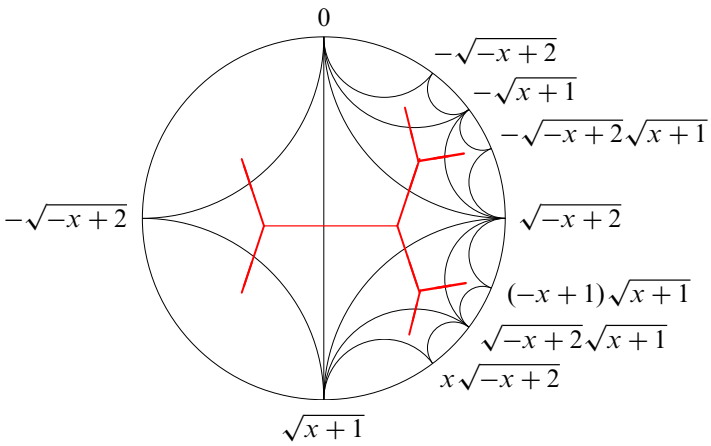

Figure 4: The Farey tessellation used to compute traces. See Section 5.0.2 for a discussion of the choice of sign of the square roots.

Suppose that (U, V, W) are the labels of regions round a vertex with $u = \operatorname{Tr}\rho(U)$, $v = \operatorname{Tr}\rho(V)$, $w = \operatorname{Tr}\rho(W)$. By (2-2), we have $u^2+v^2+w^2-uvw = \mu$. By (2-1), the two vertices opposite the ends of the edge between regions (U, V) correspond to regions UV, UV^{-1} with labels $w, uv-w$, respectively. Moving in this way, along the three edges which meet at the vertex with labels (u, v, w) to the three adjacent vertices, gives rise to the three basic moves $(u, v, w) \to (u, v, uv-w)$, $(u, v, w) \to (u, uw-v, w)$, $(u, v, w) \to (vw-u, v, w)$ which generate traces of all possible elements in Ω (and hence $\mathcal{P}$). Note that any of these three moves leaves $\operatorname{Tr}\rho([U, V])$ and hence μ invariant; in other words, μ is an invariant of the tree. Bowditch's original paper was mostly confined to the case $\mu = 0$.

In this way, the Markoff tree provides a fast way to compute traces of elements in $\mathcal{P}$ starting from an initial triple (u, v, w). This is illustrated in Figure 4 with the initial triple $(\sqrt{x+1}, 0, \sqrt{-x+2})$ which is used in Section 5.0.2. We denote the tree of traces associated to an initial triple (u, v, w) by $\mathbb{T}_{(u,v,w)}$. Later we will use a variant of this construction to compute traces of curves on a four-pointed sphere; see Section 4.4.

2.2 The Bowditch set

It is convenient to rephrase the above discussion using the terminology introduced in [3]. As above, let Ω denote the set of complementary regions of the tree $\mathbb{T}$. Define a *Markoff map* to be a map $\phi\colon \Omega \to \mathbb{C}$ such that ϕ satisfies the trace relations (2-1) and (2-2). The set of all Markoff maps is denoted by Φ. Since traces depend only on conjugacy classes, a representation $\rho\colon F_2 \to \mathrm{SL}(2, \mathbb{C})$ defines a Markoff map by

setting $\phi(U) = \operatorname{Tr}\rho(U)$ for $U \in \Omega$. Fixing once and for all an identification of Ω with $\hat{\mathbb{Q}}$ (and recalling that Ω is identified with conjugacy classes of elements in $\mathcal{P}$), we have $\phi(p/q) = \operatorname{Tr}\rho(W_{p/q})$ for $p/q \in \hat{\mathbb{Q}}$, where $W_{p/q}$ is the special word in the conjugacy class corresponding to $p/q \in \Omega$.

Thus as explained above, using the trace relations (2-1) and (2-2), an initial triple $(x, y, z) \in \mathbb{C}^3$ uniquely determines a Markoff map $\phi = \phi_{x,y,z}$ together with a corresponding labelling of $\mathbb{T}$. Conversely a Markoff map $\phi \in \Phi$ determines $(x, y, z) \in \mathbb{C}^3$ by setting $x = \phi(0/1)$, $y = \phi(1/0)$, $z = \phi(1/1)$. In this way, we can identify Φ with $\mathbb{C}^3$. For $\phi \in \Phi$, denote the corresponding tree endowed with the labelling given by ϕ by $\mathbb{T}_\phi = \mathbb{T}_{(\phi(0/1),\phi(1/0),\phi(1/1))}$.

The Bowditch set $\mathcal{B}$ is the set of all $\phi \in \Phi$ with $\mu \neq 4$ which satisfy the conditions

$$\phi(U) \notin [-2, 2] \text{ for all } U \in \Omega, \tag{2-3}$$

$$\{U \in \Omega : |\phi(U)| \leq 2\} \text{ is finite.} \tag{2-4}$$

The Bowditch set $\mathcal{B}$ is open in $\mathbb{C}^3$ and $\operatorname{Out}(F_2)$ acts properly discontinuously on $\mathcal{B}$. Furthermore, if $\phi \in \mathcal{B}$, then $\log^+ |\phi(U)| = \max\{0, \log|\phi(U)|\}$ has Fibonacci growth on Ω; see [30].

Remark 2.1 The maps ϕ for which $\mu = 4$ correspond to the reducible representations: our definition above automatically excludes them from $\mathcal{B}$. For such ϕ, there are infinitely many $U \in \Omega$ such that $|\phi(U)| < m$ for $m > 2$, they can alternatively be excluded from $\mathcal{B}$ by relaxing condition (2-4) to the condition that $\{U \in \Omega : |\phi(U)| \leq 2 + \epsilon\}$ be finite for any $\epsilon > 0$. As is easily checked from the trace relation (2-2), such representations occur in Δ precisely at the points $x = -1$, $x = 2$.

2.2.1 Background to the algorithm Our algorithm for computing which points lie in $\mathcal{B}$ is based on results from [3; 30] which we summarise here. We consider only ϕ for which $\mu \neq 4$. Following Bowditch [3], we orient the edges of $\mathbb{T}_\phi$ in the following way. Suppose that labels of the regions adjacent to some edge e are u, v, and the labels of the two remaining regions at the two end vertices are w, t; see Figure 3. From the trace relations, $t = uv - w$. Orient e by putting an arrow from t to w whenever $|t| > |w|$ and vice versa. If both moduli are equal, make either choice; if the inequality is strict, say that the edge is *oriented decisively*.

A *sink region* of $\mathbb{T}_\phi$ is a connected nonempty subtree T such that the arrow on any edge not in T points towards T decisively. A sink region may consist of a single *sink vertex* v (the three edges adjacent to v point towards v) and no edges. Clearly a sink region is not unique: one can always add further vertices and edges around the boundary of T.

For any $m \geq 0$ and $\phi \in \Phi$, define $\Omega_\phi(m) = \{U \in \Omega : |\phi(U)| \leq m\}$. The following lemmas from [30] show that $\Omega_\phi(2)$ is connected, and that from any initial vertex not adjacent to regions in $\Omega_\phi(2)$, the arrows determine a descending path through $\mathbb{T}$ which either runs into a sink, or meets vertices adjacent to regions in $\Omega_\phi(2)$. Furthermore, if $\phi(U)$ takes values away from the exceptional set $E = [-2, 2] \cup \{\pm\sqrt{\mu}\} \subset \mathbb{C}$, then there exists a finite segment of ∂U such that the edges adjacent to U not in this segment are directed towards this segment.

Lemma 2.2 [30, Lemma 3.7] *Suppose $U, V, W \in \Omega$ meet at a vertex v with the arrows on both the edges adjacent to U pointing away from v. Then either $|\phi(U)| \leq 2$ or $\phi(V) = \phi(W) = 0$.*

Corollary 2.3 [30, Theorem 3.1(2)] *Let $\phi \in \Phi$. Then $\Omega_\phi(2)$ (more generally, $\Omega_\phi(m)$ for $m \geq 2$) is connected.*

Lemma 2.4 [30, Lemma 3.11 and following comment] *Suppose β is an infinite ray consisting of a sequence of edges of $\mathbb{T}_\phi$ all of whose arrows point away from the initial vertex. Then β meets at least one region $U \in \Omega$ with $|\phi(U)| < 2$. Furthermore, if the ray does not follow the boundary of a single region, it meets infinitely many regions with this property.*

Lemma 2.5 [30, Lemma 3.20] *Suppose that $\phi(U) \notin E$, and consider the regions $V_i, i \in \mathbb{Z}$ adjacent to U in order round ∂U. Then away from a finite subset, the values $|\phi(V_i)|$ are increasing and approach infinity as $i \to \infty$ in both directions. Hence there exists a finite segment of ∂U such that the edges adjacent to U not in this segment are directed towards this segment.*

We remark that if $\phi(U) = \pm\sqrt{\mu}$ and $\sqrt{\mu} \notin [-2, 2]$, then the values of $|\phi(V_i)|$ in Lemma 2.5 approach zero in one direction round ∂U [30, Lemma 3.10], and hence $\phi \notin \mathcal{B}$ since condition (2-4) will not be satisfied. Hence, for $\phi \in \mathcal{B}$, we have $\phi(U) \notin E$ for all $U \in \Omega$.

The set $\Omega_\phi(2)$ can be used to construct a sink region T (which depends of course on ϕ) which is finite if and only if $\phi \in \mathcal{B}$. Essentially, if $\phi \in \mathcal{B}$, then T consists of finite segments of the boundaries of the (finite number of) elements of $\Omega_\phi(2)$. These are the segments alluded to in Lemma 2.5; they have to be large enough so the conclusion of the lemma holds, and also to contain all edges adjacent to any pair U, V, both of which are in $\Omega_\phi(2)$, so that the union is connected. To do this, an explicit function $H_\mu\colon \mathbb{C} \to \mathbb{R}^+ \cup \{\infty\}$ is constructed (see Lemma 3.20, the following remark and Lemma 3.23 in [30]) as follows:

(1) If $x \in E$, define $H_\mu(x) = \infty$.

(2) For $x \notin E$, let $x = \lambda + \lambda^{-1}$ with $|\lambda| > 1$ (note that $|\lambda| \neq 1$ since $x \notin [-2, 2]$). Define

$$H_\mu(x) = \max\left\{2,\ \sqrt{\left|\frac{x^2-\mu}{x^2-4}\right|}\,\frac{2|\lambda|^2}{|\lambda|-1}\right\}. \tag{2-5}$$

Then H_μ is continuous on $\mathbb{C} \setminus E$. Now we can define a specific attracting subtree:

Definition 2.6 Given $\phi \in \Phi$, let $T = T_\phi$ be the subset of $\mathbb{T}_\phi$ defined as follows:

(1) An edge with adjacent regions U, V is in T if and only if either $|\phi(U)| \leq 2$ and $|\phi(V)| \leq H_\mu(\phi(U))$, or vice versa.

(2) Any sink vertex is in T, as are any vertices which are the endpoints of two edges in T.

Based on the above lemmas, we have the following theorem (see also the special properties of the function H_μ and Lemmas 3.21–3.24 in [30]).

Theorem 2.7 *Given $\phi \in \Phi$ (with $\mu \neq 4$), the set $T = T_\phi$ in Definition 2.6 is a nonempty, connected subtree of $\mathbb{T}_\phi$. Moreover, T is a sink region for $\mathbb{T}_\phi$; that is, all edges not in T are directed decisively towards T. Furthermore, T is finite if and only if $\phi \in \mathcal{B}$.*

2.2.2 The algorithm Based on the above discussion, our algorithm to decide whether or not $\phi \in \mathcal{B}$ is as follows.

Step 1 Starting at any vertex, follow the direction of decreasing arrows. On reaching a sink vertex, stop. This vertex is in T by Definition 2.6. If the input is $\mathcal{B}$, then this method always finds a sink vertex in finite time because there is a finite sink region. Otherwise, the process may not terminate in (prespecified) finite time, and the algorithm is indecisive.

Step 2 Assuming a stopping point is found in Step 1, starting from this point, search outwards by a depth first search using Definition 2.6 to identify whether or not an edge is in T. This works because of the connectedness of T. If this search terminates in (prespecified) finite time, then $\phi_{x,y,z} \in \mathcal{B}$. Otherwise, the algorithm is indecisive.

Note that if the starting point is a sink vertex and the three adjacent edges are not in T, then T consists of just the sink vertex by the connectedness of T, hence $\phi_{x,y,z} \in \mathcal{B}$. This occurs for example for the tree $\mathbb{T}_{(x,x,x)}$ with $x \in (2, 3)$.

Figure 5 shows the Bowditch set in the diagonal slice Δ as determined by this algorithm.

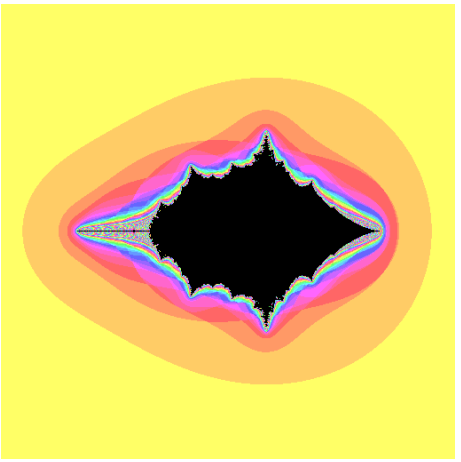

Figure 5: The Bowditch set $\mathcal{B}$ for the Markoff maps $\phi_{(x,x,x)}$, plotted in the x–plane. The grey (coloured) points are in $\mathcal{B}$ and the black ones are outside. The shades of grey (colours) indicate the size of the sink region T.

Remark 2.8 We do not have an algorithm whose output is $\phi_{x,y,z} \notin \mathcal{B}$. When $\mu = 0$, it was shown in [25] that if $|\phi(U)| \leq 0.5$ for some $U \in \Omega$, then $\phi_{x,y,z} \notin \mathcal{B}$. Hence in Step 1 above, if $\mu = 0$, we can stop when we hit a region satisfying this condition and conclude that $\phi_{x,y,z} \notin \mathcal{B}$. Using the same methods, a similar upper bound can be found for μ close to 0. In particular, there is a neighbourhood of $(0,0,0)$ which is disjoint from $\mathcal{B}$, as clearly illustrated in Figure 5. However, as shown in [11], no such universal positive bound exists for all μ: precisely, for any $\epsilon > 0$ and $\mu > 4$, there exist $\phi \in \mathcal{B}_\mu$ and $U \in \Omega$ such that $|\phi(U)| < \epsilon$. Another issue is that the sink region may be extremely large so may not be detected in a program with a given finite number of steps, this occurs when we approach the boundary of $\mathcal{B}$. Thus the algorithm is not completely decisive although it appears to give nice results. In particular, there may be false negatives; however points which are determined to be in $\mathcal{B}$ are correctly marked.

3 Groups, manifolds, symmetries and quotients

In this section we detail a construction which allows us conveniently to exploit the three-fold symmetry of groups in the diagonal slice Δ. We denote hyperbolic 3–space by $\mathbb{H}^3$ and identify its group $\mathrm{Isom}^+\,\mathbb{H}^3$ of orientation-preserving isometries with $\mathrm{PSL}(2,\mathbb{C})$. As is well known, if the image of a representation $\rho\colon F_2 \to \mathrm{SL}(2,\mathbb{C})$ is faithful, discrete and geometrically finite without parabolics, then $\mathbb{H}^3/\rho(F_2)$ is a genus-two handlebody $\mathcal{H}$; see [24, Corollary X.H.6] and also [12, Theorem 5.2]. (To apply Hempel's result, note that a hyperbolic 3–manifold is irreducible, hence prime,

and that $\pi_2(M) = 0$.) Rather than working with $\mathcal{H}$, however, it is much easier to work with the quotient $\mathcal{S}$ of $\mathcal{H}$ by the order-3 symmetry κ corresponding to cyclic permutation of the parameters. We also introduce a commensurable orbifold $\mathcal{T}$ with a torus boundary $\partial\mathcal{T}$.

Both $\mathcal{S} = \mathcal{H}/\kappa$ and $\mathcal{T}$ surject to a 3–orbifold $\mathcal{U}$ with fundamental group a so-called (P, Q, R)*–group*. Its boundary $\partial\mathcal{U}$ is a sphere with three order-2 and one order-3 cone points. A similar construction has been used extensively by Akiyoshi et al (see for example [1]), and is the basis of Wada's program OPTi [31; 32], hence was convenient for our computations. In this section we explain these constructions in detail, using them to find explicit representations of all four groups.

3.1 The handlebody and related orbifolds

The symmetric handlebody $\mathcal{H}$ can be thought of as made by gluing two solid pairs of pants each with order-3 symmetry. More precisely, take a 3–ball and choose three closed disks on the boundary, placed so as to have order-3 rotational symmetry. Gluing two such balls along the closed disks produces a handlebody $\mathcal{H}$ with the required order-three symmetry κ. Rather than write down a suitably symmetric representation of $\pi_1(\mathcal{H})$ directly, we consider first the quotient orbifold $\mathcal{S} = \mathcal{H}/\kappa$. As will be justified in retrospect when we have identified the representations explicitly, this is a ball with two cone axes around each of which the angle is $\frac{2\pi}{3}$. Its boundary $\partial\mathcal{S}$ is a sphere $\Sigma_{0;3,3,3,3}$ with four order-3 cone points. We will call $\mathcal{S}$ the *large coned ball*.

The ball $\mathcal{S}$ has a further order-4 symmetry group. Consider the two cone axes which form the singular locus of $\mathcal{S}$, together with their common perpendicular. Lifting to $\mathbb{H}^3$, we obtain a configuration invariant under the π–rotation about C, the common perpendicular to the two lifted cone axes, and also under π–rotations about a unique pair of orthogonal lines in the plane orthogonal to C passing through its midpoint O; see Section 3.2.1. Denoting these latter rotations $\bar{P}, \bar{Q} \in \mathrm{Isom}^+\,\mathbb{H}^3$, the π–rotation about C is $\bar{P}\bar{Q}$ and the entire configuration is invariant under $\langle \bar{P}, \bar{Q} \rangle = \mathbb{Z}_2 \times \mathbb{Z}_2$. Thus we obtain a further quotient orbifold $\mathcal{U} = \mathcal{S}/(\mathbb{Z}_2 \times \mathbb{Z}_2)$, also topologically a ball, which we call the *small coned ball*. The singular locus of $\mathcal{U}$ is as follows. Let $\hat{O}$ and $\hat{E}$ be the images in $\mathcal{U}$ of the midpoint O of C and the point where C meets the axis of $\bar{K}$, respectively, where $\bar{K} \in \mathrm{Isom}^+\,\mathbb{H}^3$ is one of the two order-three rotations about the pair of lifted cone axes. Let $\hat{C}$ be the image in $\mathcal{U}$ of C, so that $\hat{C}$ is a line from $\hat{O}$ to $\hat{E}$. From $\hat{O}$ emanate three mutually orthogonal lines corresponding to the order-2 axes of $\bar{P}$, $\bar{Q}$ and $\bar{P}\bar{Q}$. One of these is the line $\hat{C}$ corresponding to $\bar{P}\bar{Q}$ which ends at $\hat{E}$. From $\hat{E}$ also emanates an order-3 singular line, the axis of $\bar{K}$, perpendicular to $\hat{C}$. The boundary $\partial\mathcal{U}$ is a sphere $\Sigma_{0;2,2,2,3}$ with 3 cone points of order 2 and one of order 3. The order-3 cone point is the image of the endpoint of the

order-3 singular line and the order-2 cone points correspond to the endpoints on $\partial\mathcal{U}$ of the axes of $\bar{P}$, $\bar{Q}$ and a third involution $\bar{R}$ defined below.

Finally, there is a double cover of the small coned ball $\mathcal{U}$ by an cone manifold $\mathcal{T}$ which is topologically a solid torus. Its boundary is a torus $\partial\mathcal{T}$ with a single cone point of angle $\frac{4\pi}{3}$. Just as the quotient of a once punctured torus $\Sigma_{1;\infty}$ by the hyperelliptic involution is the surface $\Sigma_{0;2,2,2,\infty}$, so the quotient of $\partial\mathcal{T}$ by the hyperelliptic involution ι is the surface $\partial\mathcal{U} = \Sigma_{0;2,2,2,3}$. The involution ι extends to an involution, also denoted by ι, of $\mathcal{T}$ such that $\mathcal{T}/\iota = \mathcal{U}$.

The group $\pi_1(\mathcal{U})$ is generated by $(\bar{P}, \bar{Q}, \bar{K})$, where $(\bar{P}, \bar{Q}, \bar{K})$ are regarded as elements of $\mathrm{Isom}^+\,\mathbb{H}^3 = \mathrm{PSL}(2,\mathbb{C})$. We can replace $\bar{K}$ by a further involution $\bar{R}$ such that $\bar{R}\bar{Q}\bar{P} = \bar{K}$. To do this, let $\bar{R}$ be an order-2 rotation about an axis contained in the plane through E orthogonal to $\mathrm{Ax}\,\bar{K}$, such that the axis makes an angle $\frac{1}{3}\pi$ with C. (We will fix orientations more precisely below.) Then $\bar{R}(\bar{Q}\bar{P})$ is a $\frac{2\pi}{3}$–rotation about $\mathrm{Ax}\,\bar{K}$, in other words, provided orientations have been chosen correctly, we can identify $\pi_1(\mathcal{U})$ with a group

$$\langle \bar{P}, \bar{Q}, \bar{R} \mid \bar{P}^2 = \bar{Q}^2 = \bar{R}^2 = (\bar{R}\bar{Q}\bar{P})^3 = \mathrm{id},\ \bar{P}\bar{Q} = \bar{Q}\bar{P}\rangle \subset \mathrm{PSL}(2,\mathbb{C}).$$

As discussed in Remarks 3.1 and 3.2 below, the above group $\pi_1(\mathcal{U})$ cannot be lifted to a subgroup of $\mathrm{SL}(2,\mathbb{C})$ since it contains elements of order two. Nevertheless, we shall find lifts $P, Q, R \in \mathrm{SL}(2,\mathbb{C})$ of $\bar{P}, \bar{Q}, \bar{R} \in \mathrm{PSL}(2,\mathbb{C})$ for which

$$\Gamma_{\mathcal{U}} = \langle P, Q, R \mid P^2 = Q^2 = R^2 = (RQP)^3 = -\mathrm{id},\ PQ = -QP\rangle \subset \mathrm{SL}(2,\mathbb{C}),$$

so that $\Gamma_{\mathcal{U}}$ projects to $\pi_1(\mathcal{U})$.

To do this, we recall that in [1] and other papers by the same authors, groups generated by three involutions $P, Q, R \in \mathrm{SL}(2,\mathbb{C})$ with RQP parabolic, are used as a convenient way of parametrising representations of once punctured tori, where the torus in question is now a two-fold cover of the orbifold with fundamental group $\langle P, Q, R\rangle$ with quotient induced by the hyperelliptic involution. A small modification of their parametrisation allows us to write down a convenient general form for a representation of the group $\Gamma_{\mathcal{U}}$ with the presentation above into $\mathrm{SL}(2,\mathbb{C})$, from which we obtain explicit $\mathrm{SL}(2,\mathbb{C})$ representations of $\pi_1(\mathcal{H})$, $\pi_1(\mathcal{S})$, together with groups in $\mathrm{SL}(2,\mathbb{C})$ which project to $\mathrm{PSL}(2,\mathbb{C})$ representations of $\pi_1(\mathcal{U})$ and $\pi_1(\mathcal{T})$ as above. This we do in the next section.

3.2 The basic configuration and the small coned ball

We start with a general construction for representations $\Gamma_{\mathcal{U}} \to \mathrm{SL}(2,\mathbb{C})$, that is, of subgroups $\langle P, Q, R \mid P^2 = Q^2 = R^2 = (RQP)^3 = -\mathrm{id},\ PQ = -QP\rangle \subset \mathrm{SL}(2,\mathbb{C})$.

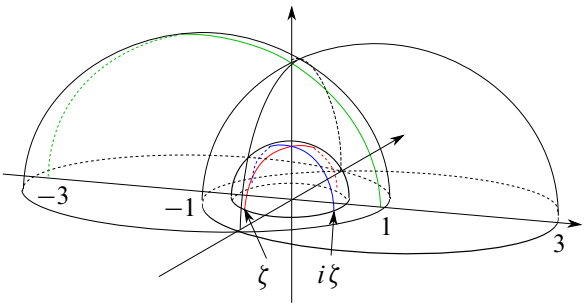

Figure 6: The basic configuration for the (P, Q, R)–group $\pi_1(\mathcal{U})$

For convenience we refer to such a group (or its image in $\mathrm{PSL}(2,\mathbb{C})$) as a (P, Q, R)–*group*. The elements P, Q, R, K we construct will project to the $\mathrm{PSL}(2,\mathbb{C})$ elements $\bar{P}, \bar{Q}, \bar{R}, \bar{K}$ discussed above.

We will make our calculations using *line matrices* following [8]. Note this will define representations into $\mathrm{SL}(2,\mathbb{C})$, thus fixing the signs of traces. Let $u, u' \in \widehat{\mathbb{C}}$, and denote the oriented line from u to u' by $[u, u']$. The associated line matrix $M([u, u']) \in \mathrm{SL}(2,\mathbb{C})$ is a matrix which induces an order two rotation about $[u, u']$ and such that $M([u, u'])^2 = -\mathrm{id}$, so that in particular,

$$M([0,\infty]) = \begin{pmatrix} i & 0 \\ 0 & -i \end{pmatrix}.$$

By [8, page 64, equation (1)], we have, if $u, u' \in \mathbb{C}$,

$$M([u, u']) = \frac{i}{u'-u} \begin{pmatrix} u+u' & -2uu' \\ 2 & -u-u' \end{pmatrix}.$$

The representation we require is derived from a basic configuration shown in Figure 6. It depends on a single parameter $\zeta \in \mathbb{C}$ which we will relate to the original parameter x in Section 3.2.3 below.

Let $\zeta \in \mathbb{C}$ and $P, Q, R \in \mathrm{SL}(2,\mathbb{C})$ be π–rotations about the oriented lines $[\zeta, -\zeta]$, $[i\zeta, -i\zeta]$ and $[1, -3]$, respectively. By construction $P^2 = Q^2 = R^2 = -\mathrm{id}$. Moreover, $\mathrm{Ax}\, P$ and $\mathrm{Ax}\, Q$ intersect at the point $|\zeta| j \in \mathbb{H}^3$ on the hemisphere of radius $|\zeta|$ and centre $0 \in \mathbb{C}$, where $z + tj$ represents the point at height $t > 0$ above $z \in \mathbb{C}$ in the upper half space model of $\mathbb{H}^3$. Thus $PQ = -QP$ and PQ is an order-2 rotation about the vertical axis $0 + tj, t > 0$.

Let V be the vertical plane above the real axis in $\mathbb{H}^3$. Note that the oriented axes of the order two rotations PQ and R both lie in V, intersecting in the point $\sqrt{3}j$ at angle $\frac{1}{3}\pi$. The line $[\sqrt{3}i, -\sqrt{3}i]$ passes through this point and is orthogonal to V. It follows that $RPQ = -RQP$ is anticlockwise rotation through $\frac{2\pi}{3}$ about the

line $[\sqrt{3}i, -\sqrt{3}i]$. Using line matrices as above, we can now easily write down the corresponding representation in $\mathrm{SL}(2,\mathbb{C})$:

$$\begin{aligned} P = M([\zeta,-\zeta]) &= -\frac{i}{2\zeta}\begin{pmatrix} 0 & 2\zeta^2 \\ 2 & 0 \end{pmatrix} = \begin{pmatrix} 0 & -i\zeta \\ -i/\zeta & 0 \end{pmatrix}, \\ Q = M([i\zeta,-i\zeta]) &= -\frac{1}{2\zeta}\begin{pmatrix} 0 & -2\zeta^2 \\ 2 & 0 \end{pmatrix} = \begin{pmatrix} 0 & \zeta \\ -1/\zeta & 0 \end{pmatrix}, \\ R = M([1,-3]) &= -\frac{i}{4}\begin{pmatrix} -2 & 6 \\ 2 & 2 \end{pmatrix} = \begin{pmatrix} i/2 & -3i/2 \\ -i/2 & -i/2 \end{pmatrix}. \end{aligned}$$

Let $K = RPQ$. Then

$$K = \begin{pmatrix} -1/2 & -3/2 \\ 1/2 & -1/2 \end{pmatrix}, \quad K^3 = \begin{pmatrix} 1 & 0 \\ 0 & 1 \end{pmatrix},$$

so that as expected, K is a anticlockwise rotation about $[\sqrt{3}i, -\sqrt{3}i]$ by $\frac{2\pi}{3}$.

Note that $P^2 = Q^2 = -\mathrm{id}$ and $PQ = -QP$ as matrices in $\mathrm{SL}(2,\mathbb{C})$. As isometries of $\mathbb{H}^3$, the signs are irrelevant. We could have chosen $K = RQP$, in which case $K^3 = -\mathrm{id}$, but see Remark 3.1 below. We denote the group generated by P, Q, R by $G_{\mathcal{U}}(\zeta)$ and the corresponding representation $\Gamma_{\mathcal{U}} \to \mathrm{SL}(2,\mathbb{C})$ by $\rho_{\mathcal{U}}(\zeta)$.

3.2.1 The large coned ball $\mathcal{S}$ To relate $\pi_1(\mathcal{U})$ to $\pi_1(\mathcal{S})$, start with two oriented axes A_0, A_1 about each of which we have order-3 anticlockwise rotations K_0, K_1, measured with respect to the orientation of the axes. Let C denoted the common perpendicular between A_0 and A_1, oriented from A_0 to A_1. We denote this configuration, which is clearly well defined up to isometry, by $\mathcal{CF}$. As described in Section 3.1, $\mathcal{CF}$ has a further $\mathbb{Z}_2 \times \mathbb{Z}_2$ group of symmetries generated by the π–rotations $\bar{P}, \bar{Q} \in \mathrm{PSL}(2,\mathbb{C})$ with axes through the mid-point of C: precisely, let Π be the plane through the mid-point of C and orthogonal to C. Then (working equivalently with the lifts $P, Q \in \mathrm{SL}(2,\mathbb{C})$) the axes of P, Q are the two lines in Π which bisect the angles between the projections of $\mathrm{Ax}\, K_0, \mathrm{Ax}\, K_1$ onto Π, chosen so that the angle bisected by $\mathrm{Ax}\, P$ is that between the projection of the lines $\mathrm{Ax}\, K_0, \mathrm{Ax}\, K_1$ with the same (say outward) orientation.

This choice of P ensures that $PK_0P^{-1} = K_1$ while $QK_0Q^{-1} = K_1^{-1}$. Also PQ is the order-2 rotation about C, and $PQK_iQ^{-1}P^{-1} = K_i^{-1}$ for $i = 0, 1$. As in Section 3.1, $\mathcal{U} = \mathcal{S}/(\mathbb{Z}_2 \times \mathbb{Z}_2)$, and we can take $\pi_1(\mathcal{U})$ to be the (P, Q, R)–group defined in Section 3.2. In terms of (P, Q, R), the generators of $\pi_1(\mathcal{S})$ are $K_0 = RPQ$, $K_1 = PK_0P^{-1}$. Thus

$$K_0 = -\begin{pmatrix} 1/2 & 3/2 \\ -1/2 & 1/2 \end{pmatrix}, \quad K_1 = -\begin{pmatrix} 1/2 & -\zeta^2/2 \\ 3/(2\zeta^2) & 1/2 \end{pmatrix}.$$

In terms of generators for $\pi_1(\partial\mathcal{S})$, we also have $K_2 = QK_0Q^{-1}$, $K_3 = RK_0R^{-1}$, where

$$K_2 = -\begin{pmatrix} 1/2 & \zeta^2/2 \\ -3/(2\zeta^2) & 1/2 \end{pmatrix}, \quad K_3 = -\begin{pmatrix} 1/2 & -3/2 \\ 1/2 & 1/2 \end{pmatrix},$$

so that $K_0K_3K_1K_2 = \mathrm{id}$.

We denote the group with generators K_0, K_1 by $G_{\mathcal{S}}(\zeta)$ and the corresponding representation $\pi_1(\mathcal{S}) \to \mathrm{SL}(2,\mathbb{C})$ by $\rho_{\mathcal{S}}(\zeta)$. From now on, we frequently drop the subscript and refer to K_0 as K.

3.2.2 The handlebody $\mathcal{H}$ We are now able to determine the images of generators X, Y of $\pi_1(\mathcal{H})$ as matrices in $\mathrm{SL}(2,\mathbb{C})$ under a suitable representation $\rho_{\mathcal{H}}(\zeta)$. To simplify notation, we shall from now on frequently identify generators of $\pi_1(\mathcal{H})$ with their images in $\mathrm{SL}(2,\mathbb{C})$, thus writing X, Y in place of $\rho_{\mathcal{H}}(\zeta)(X), \rho_{\mathcal{H}}(\zeta)(Y)$ and so on.

Observe that the generator $X \in \pi_1(\mathcal{H})$ projects to the loop represented by K_0K_1 in $\mathcal{H}/\kappa$. (This latter is a loop in $\partial\mathcal{H}/\kappa$ which separates one of each pair of the cone points of K_0, K_1 from the other pair.) We arrange that the action of κ is induced by conjugation by $K_0^{-1} = K^{-1}$, so the generators of $\pi_1(\mathcal{H})$ can be written in terms of the generators of $\pi_1(\mathcal{S})$ as $X = K_0K_1$, $Y = K_0^{-1}XK_0 = K_1K_0$. Thus we have

$$K^{-1}XK = Y, \quad K^{-1}YK = (XY)^{-1}, \quad K^{-1}(XY)^{-1}K = X.$$

Using the formulae from the previous section, this gives

$$X = \begin{pmatrix} 9/(4\zeta^2) + 1/4 & -\zeta^2/4 + 3/4 \\ 3/(4\zeta^2) - 1/4 & \zeta^2/4 + 1/4 \end{pmatrix}, \quad Y = \begin{pmatrix} \zeta^2/4 + 1/4 & -\zeta^2/4 + 3/4 \\ 3/(4\zeta^2) - 1/4 & 9/(4\zeta^2) + 1/4 \end{pmatrix}.$$

In particular this reveals the relation between the parameter ζ and x:

$$x = \mathrm{Tr}\, X = \mathrm{Tr}\, Y = \mathrm{Tr}\, XY = \frac{\zeta^2}{4} + \frac{9}{4\zeta^2} + \frac{1}{2}. \tag{3-1}$$

We denote the group with generators X, Y by $G_{\mathcal{H}}(\zeta)$ and the corresponding representation $\pi_1(\mathcal{H}) \to \mathrm{SL}(2,\mathbb{C})$ by $\rho_{\mathcal{H}}(\zeta)$; we explain in Section 3.2.5 why up to conjugation $\rho_{\mathcal{H}}(\zeta)$ in fact depends only on x.

Remark 3.1 In the above discussion, we made choices of sign so that $K^3 = \mathrm{id}$, $X = K_0K_1$ (where $K = K_0$ as above). To compute the discreteness locus of a family of representations only requires looking in $\mathrm{PSL}(2,\mathbb{C})$, however for computations involving traces we need a lift to $\mathrm{SL}(2,\mathbb{C})$.

By [6], any $\mathrm{PSL}(2,\mathbb{C})$ representation of a Kleinian group can be lifted to $\mathrm{SL}(2,\mathbb{C})$ provided there are no elements of order 2; in particular this applies to $\mathrm{PSL}(2,\mathbb{C})$ representations of $\pi_1(\mathcal{S})$ and $\pi_1(\mathcal{H})$. Since the product of the three generating loops corresponding to X, Y, Z is the identity in $\pi_1(\mathcal{H})$, we should make a choice of lift in which $XYZ = \mathrm{id}$ in $\mathrm{SL}(2,\mathbb{C})$. We could choose the element K which represents the 3–fold symmetry κ to be such that either $K^3 = \mathrm{id}$ or $K^3 = -\mathrm{id}$; however, since we intend to work with representations of $\pi_1(\mathcal{S}) \to \mathrm{SL}(2,\mathbb{C})$, we should make the choice $K^3 = \mathrm{id}$ because K corresponds to a loop round an order-3 cone axis in the quotient orbifold $\mathcal{S}$.

In the representation we have written down, we achieve $K^3 = \mathrm{id}$ with the choice $K = RPQ = \left(\begin{smallmatrix} -1/2 & -3/2 \\ 1/2 & -1/2 \end{smallmatrix}\right)$. It is easy to check that taking $K^3 = \mathrm{id}$, if we let $X = K_0 K_1$, we get $XYZ = \mathrm{id}$ as required, but if we choose $X = -K_0 K_1$, we get $XYZ = -\mathrm{id}$, which is wrong.

3.2.3 The singular solid torus $\mathcal{T}$ Finally we discuss the associated singular solid torus $\mathcal{T}$, which is constructed in a standard way from the (P, Q, R)–group. We do not logically need to use $\mathcal{T}$ in our further development, however as explained in Section 5, in practice we used $\mathcal{T}$ for computations, moreover the interpretation of the problem in the more familiar setting of a torus with a cone point may be helpful.

The boundary $\partial\mathcal{U}$ is a sphere with 4 cone points x_P, x_Q, x_R and x_K corresponding to P, Q, R and $K = RPQ$. Thus we can take as generators of $\pi_1(\mathcal{T})$ the element $B = PQ$ whose projection to $\mathcal{T}$ is a loop separating x_P, x_Q from x_R, x_K, and the element $A = RQ$ which projects to a loop separating x_R, x_Q from x_P, x_K. Since P, Q have a common fixed point, B is an order-2 elliptic, while since the axes of R, Q are (generically) disjoint, A is a loxodromic whose axis extends the common perpendicular to $\mathrm{Ax}\, R$ and $\mathrm{Ax}\, Q$.

Using the formulae above for the (P, Q, R)–group, we compute

$$RQ = A = \begin{pmatrix} 3i/(2\zeta) & i\zeta/2 \\ i/(2\zeta) & -i\zeta/2 \end{pmatrix}, \quad PQ = B = \begin{pmatrix} i & 0 \\ 0 & -i \end{pmatrix},$$

so that

$$\mathrm{Tr}\, A = \frac{3i}{2\zeta} - \frac{i\zeta}{2}, \quad \mathrm{Tr}\, B = 0, \quad \mathrm{Tr}\, AB = -\frac{\zeta}{2} - \frac{3}{2\zeta}. \tag{3-2}$$

Note that $AB = RP$ and $A^2 = -K_0 K_1$, $B^2 = -\mathrm{id}$. We also deduce that

$$ABA^{-1}B^{-1} = [A, B] = \begin{pmatrix} 1/2 & -3/2 \\ 1/2 & 1/2 \end{pmatrix}, \quad \text{so that } \mathrm{Tr}\,[A, B] = 1.$$

Note that $\operatorname{Tr} A \in [-2, 2]$ if and only if $|\zeta| = \sqrt{3}$ or $\zeta = it$ with $1 \le |t| \le 3$, justifying the above remark that generically A is loxodromic. Note also that $A^2 = -K_0 K_1$ is consistent with the direct computation using (3-2) that $\operatorname{Tr}(A^2) = -(\zeta^2/4 + 9/(4\zeta^2) + 1/2)$. Also note that $[A, B] = -K^2$, so that the commutator is rotation by $\frac{4\pi}{3}$ about $\operatorname{Ax} K$. Since $\operatorname{Tr} K^2 = (\operatorname{Tr} K)^2 - 2$, we find also that $\operatorname{Tr}[A, B] = 1$ independently of the choice of sign for K. This is consistent with $\operatorname{Tr}[A, B] = -2\cos\left(\frac{2\pi}{3}\right)$, the sign being negative by analogy with the well known fact that for any irreducible representation of a once punctured torus group for which the commutator is parabolic, we have $\operatorname{Tr}[A, B] = -2$.

We denote the group with generators A, B by $G_{\mathcal{T}}(\zeta)$ and the corresponding representation $\pi_1(\mathcal{T}) \to \mathrm{SL}(2, \mathbb{C})$ by $\rho_{\mathcal{T}}(\zeta)$.

Remark 3.2 Once again there are questions of sign which this time are a little more subtle. If $\alpha \in \mathrm{PSL}(2, \mathbb{C})$ corresponds to an element of order 2 in $\pi_1(M)$, then the corresponding representation cannot be lifted to $\mathrm{SL}(2, \mathbb{C})$, because for nontrivial $\alpha \in \mathrm{SL}(2, \mathbb{C})$, necessarily $\alpha^2 = -\mathrm{id}$; see [20] and [6]. Since in $\pi_1(\mathcal{T})$ the element B^2 is trivial, a $\mathrm{PSL}(2, \mathbb{C})$ representation of $\pi_1(\mathcal{T})$ cannot be lifted to $\mathrm{SL}(2, \mathbb{C})$. Nevertheless, we can as above write down a group in $\mathrm{SL}(2, \mathbb{C})$ which projects to a $\mathrm{PSL}(2, \mathbb{C})$ representation for $\pi_1(\mathcal{T})$. See Section 5 for further discussion on this point.

3.2.4 More on the configuration for the large coned ball $\mathcal{S}$ The relation (3-1) can be given a geometrical interpretation in terms of the perpendicular distance between the axes of K_0, K_1 which sheds light on the symmetries of the configuration $\mathcal{CF}$ in Section 3.2.1. To measure complex distance, we use the conventions spelled out in detail in [28, Section 2.1]. The signed complex distance $\boldsymbol{d}_\alpha(L_1, L_2)$ between two oriented lines L_1, L_2 along their oriented common perpendicular α is defined as follows. The signed real distance $d_\alpha(L_1, L_2)$ is the positive real hyperbolic distance between L_1, L_2 if α is oriented from L_1 to L_2 and its negative otherwise. Let $\boldsymbol{v}_i$ for $i = 1, 2$ be unit vectors to L_i at the points $L_i \cap \alpha$ and let $\boldsymbol{w}_1$ be the parallel translate of $\boldsymbol{v}_1$ along α to the point $\alpha \cap L_2$. Then $\boldsymbol{d}_\alpha(L_1, L_2) = \delta_\alpha(L_1, L_2) + i\theta$ where θ is the angle, mod $2\pi i$, from $\boldsymbol{w}_1$ to $\boldsymbol{v}_2$ measured anticlockwise in the plane spanned by $\boldsymbol{w}_1$ to $\boldsymbol{v}_2$ and oriented by α.

Let σ be the signed complex distance from the *oriented* axis $\operatorname{Ax} K_0$ to the oriented axis $\operatorname{Ax} K_1$, measured along the common perpendicular C oriented from $\operatorname{Ax} K_0$ to $\operatorname{Ax} K_1$. Then $\operatorname{Ax} K_0, \operatorname{Ax} K_1$ together with $\operatorname{Ax} K_0 K_1$ form the alternate sides of a right angled skew hexagon whose other three sides are the common perpendiculars between the three axes taken in pairs. The cosine formula gives σ in terms of the complex half translation lengths $\lambda_0, \lambda_1, \lambda_2$ of K_0, K_1 and $K_0 K_1$, respectively. To get the sides oriented consistently round the hexagon, we have to reverse the orientation of

$\operatorname{Ax} K_0$ so that the complex distance σ should be replaced by $\sigma' = \sigma + i\pi$ and λ_0 by $\lambda_0' = -\lambda_0$ (see [28]), so the formula gives

$$\cosh \sigma' = \frac{\cosh \lambda_2 - \cosh \lambda_0' \cosh \lambda_1}{\sinh \lambda_0' \sinh \lambda_1}.$$

As in Section 3.2.2, we have $X = K_0 K_1$ so $x = \operatorname{Tr} K_0 K_1 = 2\cosh \lambda_2$ while for $i = 0, 1$ we have $\cosh \lambda_i = \cos \frac{2\pi}{3} = -\frac{1}{2}$ and $\sinh \lambda_i = i \sin \frac{2\pi}{3} = \frac{1}{2} i\sqrt{3}$. (Note that since K_0, K_1 are conjugate we should take $\lambda_0 = \lambda_1$ so the possible additive ambiguity of $i\pi$ in the definition of the λ_i does not change the resulting equation.) Substituting, we find

$$-\cosh \sigma = \frac{x/2 - 1/4}{(\sqrt{3}/2)^2} = \tfrac{1}{3}(2x - 1). \tag{3-3}$$

We can also relate σ directly to our parameter ζ. By construction $\operatorname{Ax} K_0$ is the oriented line $[-\sqrt{3}i, \sqrt{3}i]$, while $K_1 = P K_0 P^{-1}$ so that $\operatorname{Ax} K_1$ is the oriented line $[i\zeta^2/\sqrt{3}, -i\zeta^2/\sqrt{3}]$ and C is the oriented line from ∞ to 0. Thus the real part of the hyperbolic distance from $\operatorname{Ax} K_0$ to $\operatorname{Ax} K_1$ is $2\log \sqrt{3}/|\zeta|$, and the anticlockwise angle, measured in the plane oriented *downwards* along the vertical axis C, is $-(\pi + 2 \operatorname{Arg} \zeta)$. Hence

$$\sigma = 2\log \frac{\sqrt{3}}{|\zeta|} - 2i \operatorname{Arg} \zeta - i\pi = 2\log \frac{\sqrt{3}}{\zeta}.$$

Comparing to (3-3), we find

$$\left[\left(\frac{\sqrt{3}}{\zeta}\right)^2 + \left(\frac{\zeta}{\sqrt{3}}\right)^2\right] = 2\cosh(\sigma + i\pi) = \tfrac{2}{3}(2x - 1),$$

or

$$x - \frac{1}{2} = \frac{3}{4}\left[\left(\frac{\sqrt{3}}{\zeta}\right)^2 + \left(\frac{\zeta}{\sqrt{3}}\right)^2\right], \tag{3-4}$$

recovering and giving a more satisfactory geometrical meaning to (3-1).

3.2.5 Dependence on x versus ζ It is not perhaps immediately obvious why the groups $G_{\mathcal{S}}(\zeta), G_{\mathcal{H}}(\zeta)$ as defined above depend up to conjugation only on our original parameter x. This is clarified by the above discussion, because up to conjugation $G_{\mathcal{S}}(\zeta)$ depends only on the configuration $\mathcal{CF}$ and hence on σ which is related to x as in (3-3). An alternative way to see this is the discussion on computing traces in Section 4.4. Thus from now on, we shall alternatively write $G_{\mathcal{S}}(x), G_{\mathcal{H}}(x)$ in place of $G_{\mathcal{S}}(\zeta), G_{\mathcal{H}}(\zeta)$.

3.2.6 Symmetries The discussion in Section 3.2.4 gives insight into various symmetries of the parameters x and ζ. Equation (3-1) shows that the map $\zeta \mapsto x$ is a 4–fold covering with branch points at $\zeta = \pm\sqrt{3}$, $\zeta = \pm i\sqrt{3}$ and $z = 0, \infty$. Correspondingly, we have a Klein 4–group $\mathbb{Z}_2 \times \mathbb{Z}_2$ of symmetries which change ζ but not x:

(1) Replacing ζ by $-\zeta$ leaves the basic construction unchanged but the line matrices defining P, Q change sign.

(2) Replacing ζ by $-3/\zeta$ is an order-2 rotation about the axis $[-\sqrt{3}i, \sqrt{3}i]$. This fixes K_0 and moves K_1 into a position on the opposite side of K_0 along the vertical line C. This changes nothing other than the position we choose for the basic configuration in Section 3.2. Note however that the line matrices defining P, Q change sign.

There is also a symmetry which changes x as well as ζ. Say we fix the orientation of one of the two axes $\operatorname{Ax} K_0, \operatorname{Ax} K_1$ while reversing the other. On the level of the configuration $\mathcal{CF}$ from Section 3.2.1, this interchanges P and Q. Since $PK_0P^{-1} = K_1$ while $QK_0Q^{-1} = K_1^{-1}$, this is equivalent to fixing the orientation of one of the two axes $\operatorname{Ax} K_0, \operatorname{Ax} K_1$ while reversing the other. This symmetry interchanges the marked group P, Q, R with the marked group Q, P, R, so that one group is discrete if and only if so is the other. In terms of our parameters, the complex distance σ between the axes changes to $\sigma + i\pi$, so that $\cosh\sigma \mapsto -\cosh\sigma$ giving the symmetry $\left(x - \frac{1}{2}\right) \mapsto -\left(x - \frac{1}{2}\right)$ of (3-3). Note that the diagonal slice of the Bowditch set $\Delta \cap \mathcal{B}$ does not possess this symmetry. Interchanging P and Q is induced by the map $\zeta \mapsto i\zeta$; more precisely this map sends P to Q and Q to $-P$. This clearly induces the same symmetry in Equation (3-1). Note that by the definition, in this symmetry R remains unchanged.

On the level of the torus group $\pi_1(\mathcal{T})$, we have by definition $RQ = A$, $PQ = B$ so that $AB = RP$. Thus sending P to Q and Q to $-P$ while fixing R sends B to $-B$ and A to $-AB$. (Recall that on the level of matrices, $PQ = -QP$.) The symmetry should therefore replace the trace triple $(\operatorname{Tr} A, \operatorname{Tr} B, \operatorname{Tr} AB)$ by the triple $(-\operatorname{Tr} AB, -\operatorname{Tr} B, \operatorname{Tr} A)$. It is easily checked from (3-2) that this is exactly the change effected by $\zeta \mapsto i\zeta$.

Finally, we have the symmetry of complex conjugation induced by $x \to \overline{x}$ or equivalently $\zeta \mapsto \overline{\zeta}$. This sends $\sigma \mapsto \overline{\sigma}$ thus replacing $G_{\mathcal{H}}(x)$ by a conjugate group in which the distance between $\operatorname{Ax} K_0$ and $\operatorname{Ax} K_1$ is unchanged but the angle measured along their common perpendicular changes sign. Clearly these are different groups but one is discrete if and only if the same is true of the other.

The diagonal slice of the Bowditch set obviously also enjoys the symmetry by conjugation, however, that is its only symmetry. In particular $(x, x, x) \to (-x, -x, -x)$ is not a symmetry and the corresponding $\mathrm{SL}(2, \mathbb{C})$ representations project to different

representations of F_2 into $\mathrm{PSL}(2,\mathbb{C})$. This is because any two distinct lifts of a representation from $\mathrm{PSL}(2,\mathbb{C})$ to $\mathrm{SL}(2,\mathbb{C})$ differ by multiplying exactly two of the parameters x, y, z by -1. The allowed replacement $X \to -X$ and $Y \to -Y$ gives the group $(-x,-x,x)$ with parameters which are not in the diagonal slice Δ.

The symmetries can be seen in our plots by comparing Figure 5, the Bowditch set for the triple $\phi_{(x,x,x)}$ in the x–plane, with the right-hand frame of Figure 13, which shows the same set in the ζ–plane. Note the symmetry of complex conjugation in both pictures. In addition, Figure 13 is invariant under the maps $\zeta \mapsto -\zeta$ and $\zeta \mapsto -3/\zeta$, neither of which are seen in Figure 5. Thus the upper half plane in Figure 13 is a 4–fold covering of the upper half plane in Figure 5: as is easily checked from (3-1), the imaginary axis in Figure 13 maps to the negative real axis in Figure 5 while the real axis in Figure 13 maps to the positive real axis in Figure 5. In particular, note the following branch points and special values: if $x = 3$, then $\zeta = \pm 1, \pm 3$; if $x = 2$, then $\zeta = \pm\sqrt{3}$; if $x = -1$, then $\zeta = \pm\sqrt{3}i$; if $x = -2$, then $\zeta = \pm i, \pm 3i$.

Finally, the symmetry $\left(x - \frac{1}{2}\right) \mapsto -\left(x - \frac{1}{2}\right)$ is not visible in either picture because it does not preserve the property of lying in the Bowditch set. As we shall see later, this symmetry is visible in pictures of the discreteness locus; see the upper frame of Figure 8.

4 Discreteness

We now turn to the question of finding those values of the parameter x for which representation $\rho_x\colon F_2 \to \mathrm{SL}(2,\mathbb{C})$ is faithful with discrete geometrically finite image, where as usual $F_2 = \langle X, Y \mid - \rangle$. Let $\mathcal{D}_\mathcal{S}, \mathcal{D}_\mathcal{H} \subset \mathbb{C}$ denote the subsets of the complex x–plane on which the representations $\rho_\mathcal{S}(x), \rho_\mathcal{H}(x)$ are respectively faithful and $G_\mathcal{S}(x), G_\mathcal{H}(x)$ are discrete and geometrically finite. (See Section 3.2.5 for the replacement of $G_\mathcal{S}(\zeta), G_\mathcal{H}(\zeta)$ by $G_\mathcal{S}(x), G_\mathcal{H}(x)$.) We first show that $\mathcal{D}_\mathcal{S} = \mathcal{D}_\mathcal{H}$.

We begin with the easy observation that since all the groups in Section 3 are commensurable, they are either all discrete or all nondiscrete together:

Lemma 4.1 *Suppose that G, H are subgroups of $\mathrm{PSL}(2,\mathbb{C})$ with $G \supset H$ and that $[G : H]$ is finite. Then G is discrete (geometrically finite) if and only if the same is true of H.*

Proof If G is discrete, clearly so is H. Suppose that H is discrete but G is not. Then infinitely many distinct orbit points in $G \cdot O$ accumulate in some compact set $D \subset \mathbb{H}^3$. Label the cosets of $[G : H]$ as $g_1 H, \dots, g_k H$. Then for some i there are infinitely many points $g_i h_r \cdot O \in D$, which gives infinitely many distinct points $h_r \in g_i^{-1} D$. This contradicts discreteness of H. The proof for geometric finiteness is equally straightforward. □

Lemma 4.2 *The representation $\rho_{\mathcal{S}}(x)\colon \pi_1(\mathcal{S}) \to G_{\mathcal{S}}(x)$ is faithful if and only if the same is true of $\rho_{\mathcal{H}}(x)\colon \pi_1(\mathcal{H}) \to G_{\mathcal{H}}(x)$.*

Proof Note that $\pi_1(\mathcal{S})$ is isomorphic to $\mathbb{Z}/3\mathbb{Z} * \mathbb{Z}/3\mathbb{Z} = \langle k_0, k_1 \mid k_0^3 = k_1^3 = \mathrm{id}\rangle$, while $\pi_1(\mathcal{H})$ is the subgroup of $\pi_1(\mathcal{S})$ generated by k_0k_1 and k_1k_0, and is isomorphic to a free group of rank 2. By construction, $\rho_{\mathcal{H}}(x)$ is the restriction of $\rho_{\mathcal{S}}(x)$ to $\pi_1(\mathcal{H})$. Thus, if $\rho_{\mathcal{S}}(x)$ is faithful, then so is $\rho_{\mathcal{H}}(x)$.

Now $\pi_1(\mathcal{H})$ has index three in $\pi_1(\mathcal{S})$ and $\pi_1(\mathcal{S}) = \pi_1(\mathcal{H}) \cup k_0\pi_1(\mathcal{H}) \cup k_0^{-1}\pi_1(\mathcal{H})$. Suppose that $\rho_{\mathcal{H}}(x)$ is faithful but $\rho_{\mathcal{S}}(x)$ is not. Then there exists $g \in \pi_1(\mathcal{S})$ such that $\rho_{\mathcal{S}}(x)(g) = \mathrm{id}$. Now $g = k_0^e h$, where $e = \pm 1$ and $h \in \pi_1(\mathcal{H})$. Thus $\mathrm{id} = \rho_{\mathcal{S}}(x)(g) = \rho_{\mathcal{S}}(x)(k_0^e)\rho_{\mathcal{H}}(x)(h)$ so that $\rho_{\mathcal{H}}(x)(h^3) = \rho_{\mathcal{S}}(x)(k_0^{-3e}) = \mathrm{id}$, contradicting the assumption that $\rho_{\mathcal{H}}(x)$ is faithful. □

Corollary 4.3 *The representations $\rho_{\mathcal{S}}(x), \rho_{\mathcal{H}}(x)$ are faithful, discrete and geometrically finite together; that is, $\mathcal{D}_{\mathcal{S}} = \mathcal{D}_{\mathcal{H}}$.*

Thus we may write $\mathcal{D} = \mathcal{D}_{\mathcal{S}} = \mathcal{D}_{\mathcal{H}}$. Our next aim is to find $\mathcal{D} \subset \mathbb{C}$.

4.1 Fundamental domains

We can make a rough estimate for $\mathcal{D}$ by exhibiting a fundamental domain for $G_{\mathcal{S}}(x)$ for sufficiently large x.

Proposition 4.4 *Writing $x = u + iv$, the region $\mathcal{D}$ contains the region outside the ellipse $\frac{1}{25}(2u-1)^2 + \frac{1}{4}v^2 = 1$ in the x–plane.*

Proof In view of Corollary 4.3, we can work with the large cone manifold $\mathcal{S}$ with generators K_0, K_1 of Section 3.2.1. The axis of K_0 is the line $[-i\sqrt{3}, i\sqrt{3}]$ passing through $j\sqrt{3}$. Let H, H' be the hemispheres which meet $\mathbb{R}$ orthogonally at points $-3, 1$ and $-1, 3$, respectively, and let E, E' be the closed half spaces they cut out which contain 0. Then H, H' intersect in $\mathrm{Ax}\, K_0$, moreover $E \cap E'$ is a fundamental domain for the group $\langle K_0\rangle$ acting on $\mathbb{H}^3$.

Recalling that P is the π–rotation about the line $[-\zeta, \zeta]$ which bisects the common perpendicular between $\mathrm{Ax}\, K_0$ and $\mathrm{Ax}\, K_1$, we see that the images of H, H' under P meet along $\mathrm{Ax}\, K_1$. Since $P(z) = \zeta^2/z$ for $z \in \mathbb{C}$, we have that $P(H), P(H')$ meet $P(\mathbb{R})$ orthogonally in points $-\frac{1}{3}\zeta^2, \zeta^2$ and $\frac{1}{3}\zeta^2, -\zeta^2$, respectively. If F, F' are the half spaces cut out by $P(H), P(H')$ which contain $\infty = P(0)$ (so that $F = P(E)$), then in a similar way, $F \cap F'$ is a fundamental domain for $\langle K_1\rangle$.

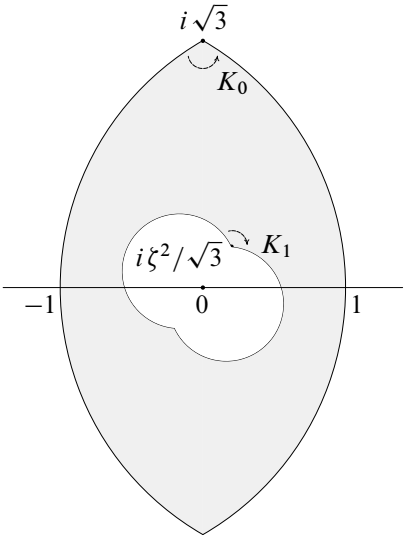

Figure 7: The shaded region illustrates the fundamental domain for $\pi_1(\mathcal{S})$ acting in its regular set in $\widehat{\mathbb{C}}$ when $|\zeta| < 1$, so that x is outside the ellipse of Proposition 4.4.

Thus if $|\zeta| < 1$, then the hemisphere of radius $|\zeta|$ centred at 0 separates the regions $(E \cap E')^C$ and $(F \cap F')^C$. We conclude by Poincaré's theorem (or a suitable simple version of the Klein–Maskit combination theorem) that in this situation the region $(E \cap E') \cap (F \cap F')$ is a fundamental domain for $\langle K_0, K_1 \rangle$, which moreover is discrete with presentation $\langle K_0, K_1 \mid K_0^3 = K_1^3 = \mathrm{id} \rangle$. Thus the representation $\rho_{\mathcal{S}}(x)$ with $x = x(\zeta)$ as in (3-1), is faithful, and hence $x \in \mathcal{D}$.

Suppose that $\zeta = e^{i\phi}$. Then from (3-3), $\frac{1}{3}(2x-1) = \cosh\sigma = \frac{1}{2}\big(\frac{1}{3}e^{2i\phi} + 3e^{-2i\phi}\big)$ so that $x = u + iv$ lies on the ellipse $\frac{1}{25}(2u-1)^2 + \frac{1}{4}v^2 = 1$ as claimed. □

The configuration when $x \in \mathbb{R}$ is of particular interest since in this case $G_{\mathcal{H}}(x)$ is Fuchsian. The ellipse meets the real axis in points $-2, 3$ so that $G_{\mathcal{H}}(x)$ is discrete and the representation is faithful on $(\infty, -2]$ (corresponding to $|\zeta| > 1$, $\zeta \in i\mathbb{R}$) and $[3, \infty)$ (corresponding to $|\zeta| > 1, \zeta \in \mathbb{R}$). In these two cases the fundamental domains look the same; see Figure 11. Note that the interval $(-2, 3)$ is definitely not in $\mathcal{D}$: if $-2 < x < 2$, then $K_0 K_1$ is elliptic since $x = \mathrm{Tr}\, K_0 K_1$, while if $-1 < x < 3$, then $K_0 K_1^{-1}$ is elliptic since $\mathrm{Tr}\, K_0 K_1^{-1} = 1 - x$; see also Section 4.5.

In the general case, a fundamental domain can be found by a modification of Wada's program OPTi [31; 32]. This program allows one to compute the limit set and fundamental domains for the PQR–group $G_{\mathcal{U}}$. A short Python program for doing this is available at `http://vivaldi.ics.nara-wu.ac.jp/~yamasita/DiagonalSlice/`.

4.2 The method of pleating rays

To determine $\mathcal{D}$, we use the Keen–Series method of pleating rays applied to the large coned sphere $\mathcal{S}$. This is closely analogous to the problem of computing the Riley slice of Schottky space, that is the parameter space of discrete geometrically finite groups freely generated by two parabolics, which was solved in [15; 19].

We begin by briefly summarising the elements of pleating ray theory we need. For more details see various of the first author's papers, for example [15; 5].

Suppose that $G \subset \mathrm{SL}(2,\mathbb{C})$ is a geometrically finite Kleinian group with corresponding orbifold $M = \mathbb{H}^3/G$ and let $\mathcal{C}/G$ be its convex core, where $\mathcal{C}$ is the convex hull in $\mathbb{H}^3$ of the limit set of G; see [7]. Then $\partial\mathcal{C}/G$ is a convex pleated surface (see for example [7]) also homeomorphic to ∂M. The bending of this pleated surface is recorded by means of a measured geodesic lamination, the *bending lamination* $\beta = \beta(G)$, whose support forms the bending lines of the surface and whose transverse measure records the total bending angle along short transversals. We say β is *rational* if it is supported on closed curves: note that closed curves in the support of β are necessarily simple and pairwise disjoint. If a bending line is represented by a curve $\gamma \in \pi_1(\mathcal{S})$, then by definition it is the projection of a geodesic axis to $\partial\mathcal{C}/G$, so in particular β contains no peripheral curves in its support. Note that any two homotopically distinct nonperipheral simple closed curves on $\partial\mathcal{S}$ intersect. Thus in this case, β is rational only if its support is a single simple essential nonperipheral closed curve on $\partial\mathcal{C}/G$.

As above, we parametrise representations $\rho_{\mathcal{S}}(x)\colon \pi_1(\mathcal{S}) \to \mathrm{SL}(2,\mathbb{C})$ by $x \in \mathbb{C}$ and denote the image group by $G_{\mathcal{S}}(x)$. From now on, we frequently write ρ_x for $\rho_{\mathcal{S}}(x)$.

Definition 4.5 Let γ be a homotopy class of simple essential nonperipheral closed curves on $\partial\mathcal{S}$. The *pleating ray* $\mathcal{P}_\gamma$ of γ is the set of points $x \in \mathcal{D}$ for which $\beta(G_{\mathcal{S}}(x)) = \gamma$.

Such rays are called *rational pleating rays*; a similar definition can be made for general projective classes of bending lamination; see [5].

The following key lemma is proved in [5, Proposition 4.1]; see also [14, Lemma 4.6]. The essence is that because the two flat pieces of $\partial\mathcal{C}/G$ on either side of a bending line are invariant under translation along the line, the translation can have no rotational part.

Lemma 4.6 *If the axis of $g \in G$ is a bending line of $\partial\mathcal{C}/G_{\mathcal{S}}(x)$, then* $\operatorname{Tr} g(x) \in \mathbb{R}$.

Notice that the lemma applies even when the bending angle θ_γ along γ vanishes, so the corresponding surface is flat, or when the angle is π, in which case either γ is parabolic or $G_{\mathcal{S}}(x)$ is Fuchsian.

If $g \in G$ represents a curve γ on $\partial\mathcal{S}$, define the *real trace locus* $\mathbb{R}_\gamma$ of γ to be the locus of points in $\mathbb{C}$ for which $\operatorname{Tr} g \in (-\infty,-2]\cup[2,\infty)$. By the above lemma, $\mathcal{P}_\gamma \subset \mathbb{R}_\gamma$.

Our aim is to compute the locus of faithful discrete geometrically finite representations $\mathcal{D}_\mathcal{S} = \mathcal{D}$. In summary, we do this as follows:

(1) Show that up to homotopy in $\mathcal{S}$, the essential nonperipheral curves on $\partial\mathcal{S}$ are indexed by $\mathbb{Q}/\sim$, where $p/q \sim \pm(p+2kq)/q$ for $k \in \mathbb{Z}$ (Proposition 4.9).

(2) Given $\gamma \in \pi_1(\partial\mathcal{S})$, give an algorithm for computing $\operatorname{Tr}\rho_x(\gamma)$ as a polynomial in x, in particular identifying its two highest order terms in terms of p, q (Section 4.4 and Proposition 4.11).

(3) Show that $\mathcal{P}_{0/1} = (-\infty,-3]$ and $\mathcal{P}_{1/1} = [2,\infty)$ (where $\mathcal{P}_{p/q}$ denotes the pleating ray of the curve $\gamma_{p/q} \in \pi_1(\partial\mathcal{S})$ identified with p/q) (Section 4.5).

(4) Show $\mathcal{P}_{p/q}$ is a union of connected nonsingular branches of $\mathbb{R}_\gamma$ (Theorem 4.14).

(5) For $p, q \neq 0, 1$, identify $\mathcal{P}_{p/q}$ by showing it has two connected components, namely the branches of $\mathbb{R}_\gamma$ which are asymptotic to the directions $e^{\pm i\pi(p/q+1)}$ as $|x| \to \infty$ (Proposition 4.20).

(6) Prove that rational rays $\mathcal{P}_{p/q}$ are dense in $\mathcal{D}_\mathcal{S}$ (Theorem 4.23).

One could carry all this out following almost word for word the arguments in [15]. Rather than do this, we indicate as appropriate how more general results can be put together to provide a somewhat less ad hoc proof of the results. The claim that $\mathcal{P}_{p/q}$ has two connected components appears to contradict the results in [15]; see however the following remark and Proposition 4.20 below. The pleating rays are shown on the top in Figure 8 with the Riley slice rays from [15] below for comparison.

Remark 4.7 There were two rather subtle errors in [15]. The first was that, in the enumeration of curves on $\partial\mathcal{S}$, we omitted to note that $\gamma_{p/q}$ is homotopic to $\gamma_{-p/q}$ in $\mathcal{S}$. The second was, that we found only one of the two components of $\mathcal{P}_{p/q}$. Since $\mathcal{P}_{p/q} = \mathcal{P}_{-p/q}$, these two errors in some sense cancelled each other out. They were discussed at length and resolved in [19] and we make corresponding corrections here.

Remark 4.8 The space of all faithful discrete representations is known to be the closure of the geometrically finite ones by the tameness and density theorems; see [23] for a detailed overview of this and other facts about deformation spaces. However these issues are not the main point of concern to us here.

4.3 Step 1: Enumeration of curves on $\partial\mathcal{S}$

We need to enumerate essential nonperipheral unoriented simple curves on $\partial\mathcal{S}$ up to free homotopy equivalence in $\mathcal{S}$. As is well known, such curves on $\partial\mathcal{S}$ are, up to free

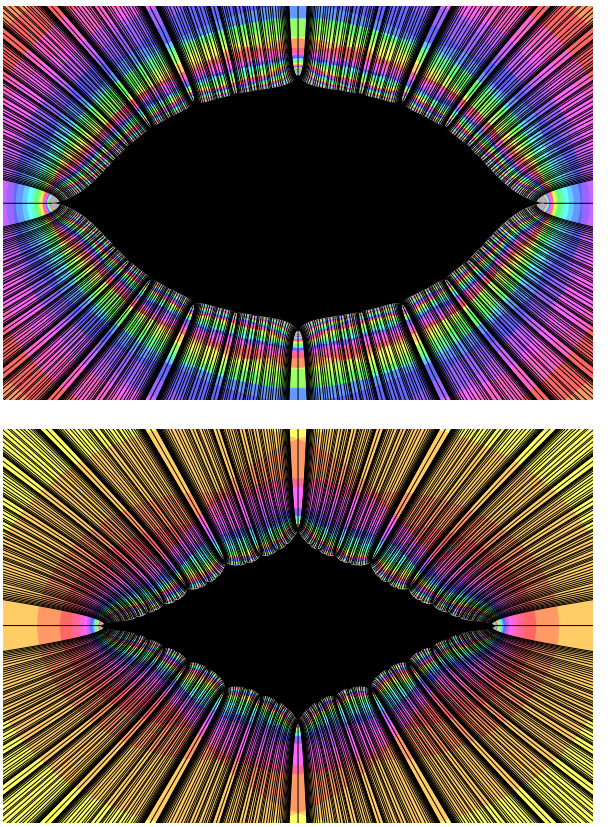

Figure 8: Top: pleating rays for $G_{\mathcal{S}}(x)$. Bottom: pleating rays for the Riley slice as described in [15]. The underlying colours indicate the Bowditch sets for the initial triples discussed in Section 5.0.3; conjecturally these coincide with the closure of the regions filled by the pleating rays. For a discussion of how the rays were actually computed; see Section 5.0.2

homotopy equivalence in $\partial\mathcal{S}$, in bijective correspondence with lines of rational slope in the plane, that is, with $\mathbb{Q}\cup\infty$; see for example [15; 19]. For (p,q) relatively prime and $q\geq 0$, denote the class corresponding to p/q by $\gamma_{p/q}$. We have:

Proposition 4.9 [19, Theorem 1.2] *The unoriented curves $\gamma_{p/q},\gamma_{p'/q'}$ are freely homotopic in $\mathcal{S}$ if and only if $p'/q'=\pm p/q+2k$ for $k\in\mathbb{Z}$.*

Missing the identification $\gamma_{p/q}\sim\gamma_{-p/q}$ was the first of the two errors in [15] referred to in Remark 4.7.

Before proving the proposition, we need to explain the identification of curves on $\partial\mathcal{S}$ with $\mathbb{Q}\cup\infty$. In [15; 19] this was done using the plane punctured at integer points as

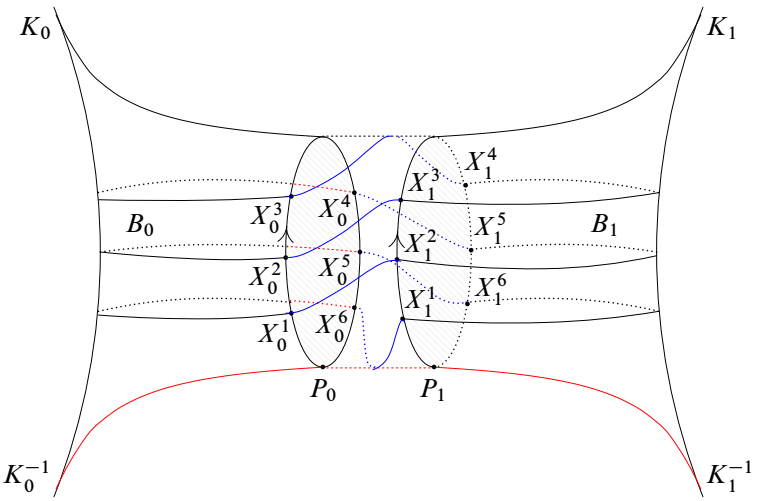

Figure 9: The arrangement of arcs on $\partial\mathcal{S}$. The curve shown illustrates the case $p = 1, q = 3$.

an intermediate covering between $\partial\mathcal{S}$ and its universal cover. The idea is sketched in Section 5.0.1. Here we give a slightly different description of the curve $\gamma_{p/q}$ which leads to a nice proof of the above result.

Cut $\mathcal{S}$ into two halves along the meridian disk m which is the projection of the plane which perpendicularly bisects the common perpendicular C to the two singular axes $\mathrm{Ax}\, K_i$ for $i = 0, 1$. Each half is a ball $\widehat{B}_i$ with a singular axis $\mathrm{Ax}\, K_i$. The boundary $\partial B_i = \partial\widehat{B}_i \cap \partial\mathcal{S}$ is a sphere with two cone points and a hole ∂m. Since the axes of K_i are oriented, we can distinguish one cone point on each ∂B_i as the positive end of $\mathrm{Ax}\, K_i$. Now $\partial\mathcal{S}$ has a hyperbolic structure inherited from the ordinary set (or from the pleated surface structure on $\partial\mathcal{C}/G_{\mathcal{S}}(x)$), in which ∂m is geodesic. With respect to such a structure, each ∂B_i has a reflectional symmetry ι in the (projection of the) plane containing $\mathrm{Ax}\, K_i$ and C, which maps the cone points to themselves, and which maps the "front" to the "back" as shown in Figure 9. There is a preferred base point P_i on ∂m, namely the foot of the perpendicular from the negative end of $\mathrm{Ax}\, K_i$ to ∂m.

Let γ be an essential nonperipheral simple curve on $\partial\mathcal{S}$, which we may assume has minimal intersection in its isotopy class with ∂m. Then $\gamma \cap \partial B_i$ consists of q arcs joining ∂m to itself for each $i = 0, 1$. On each B_i separately, after suitable isotopies, we may arrange the strands of γ symmetrically with respect to ι, that is, with front to back symmetry. However, these two isotopies may not be consistent, that is, they may not glue together to form an isotopy of ∂S. We reconstruct the gluing as follows.

Orient ∂m so that it points "upwards" on the front side of the figure. Lifting ∂m to its cyclic cover $\mathbb{R}$, enumerate in order the endpoints $X_i^k, i = 0, 1; k \in \mathbb{Z}$ of arcs of γ starting (say) with the arc meeting ∂m nearest P_i, and so that increasing order is in the direction of the upwards orientation of ∂m viewed from the front side in the figure. Since $X_i^k = X_i^{k+2q}$, the enumeration is really mod $2q\mathbb{Z}$.

To reconstruct γ we have to join the endpoints X_0^k on ∂B_0 to the endpoints $X_1^{k'}$ on ∂B_1. Since the arcs have to be matched in order round ∂m, if X_0^i is joined to X_1^j, then X_0^{i+k} is joined to X_1^{j+k} for all $k \in \mathbb{Z}$. Set $p = j - i$. Clearly this gluing can be implemented by an isotopy in an annular neighbourhood of ∂m, which can be extended to an isotopy of the whole of $\mathcal{S}$ compatible with the previous isotopies on ∂B_i.

It is not hard to see that the resulting curve $\gamma_{p/q}$ is connected if and only if (p, q) are relatively prime. Note that with this description, ∂m is the curve $q = 0$, that is, $\gamma_{1/0}$. The curve $\gamma_{0/1}$ is represented by K_0K_1 and $\gamma_{1/1}$ by $K_0K_1^{-1}$. We leave it to the reader to see that this description is the same as that obtained from the lattice picture in [15]; see also Section 5.0.1.

Notation From now on, to simplify notation, for $\gamma \in \pi_1(\mathcal{S})$ and $Z \in \mathrm{SL}(2, \mathbb{C})$, we write $\gamma \leftrightarrow Z$ to indicate that the matrix Z corresponds to the geodesic in the free homotopy class of γ under the representation $\rho_{\mathcal{S}}(x)$. Thus in particular, $\gamma_{0/1} \leftrightarrow K_0K_1$ and $\gamma_{1/1} \leftrightarrow K_0K_1^{-1}$.

Proof of Proposition 4.9 Write $\gamma_{p/q} \sim \gamma_{p'/q'}$ to indicate that $\gamma_{p/q}, \gamma_{p'/q'}$ are homotopic in $\mathcal{S}$. Since Dehn twisting round ∂m is trivial in $\mathcal{S}$ and sends $X_i^k \to X_i^{k+2q}$, we have $\gamma_{p/q} \sim \gamma_{p/q+2}$. To see why $\gamma_{p/q} \sim \gamma_{-p/q}$, first note that the result does not depend on the relative twisting between $\mathrm{Ax}\, K_0, \mathrm{Ax}\, K_1$. Thus we shall consider the case in which $\sigma \in \mathbb{R}$ (recall that σ is the complex distance between these two axes), so that $\mathrm{Ax}\, K_0, \mathrm{Ax}\, K_1$ are coplanar and point in the same "vertical" direction as in Figure 9.

Consider the orientation-reversing symmetry r of reflection in the "horizontal" plane of Figure 9, that is the plane containing C orthogonal to the two axes $\mathrm{Ax}\, K_0, \mathrm{Ax}\, K_1$. (This is where we use that $\sigma \in \mathbb{R}$.) Clearly, this symmetry sends $\gamma_{p/q}$ to $\gamma_{-p/q}$. Fixing an orientation on $\partial\mathcal{S}$, let $\alpha, \beta, \gamma, \delta$ be anticlockwise loops on $\partial\mathcal{S}$ around the four cone points represented by the projections of the positive endpoints of the (oriented) axes of $K_0, K_0^{-1}, K_1, K_1^{-1}$, respectively, so that $\alpha\beta\gamma\delta = \mathrm{id}$ and $\alpha, \beta, \gamma, \delta$ generate $\pi_1(\partial S)$. Since r reverses orientation on $\partial\mathcal{S}$ it sends an anticlockwise loop round the positive endpoint of K_0 to a clockwise loop round the negative endpoint of K_0, which is the positive endpoint of the oriented axis of K_0^{-1}. Thus $r(\alpha) = \beta^{-1}$, and

likewise $r(\gamma)=\delta^{-1}$. Since $\alpha=\beta^{-1}\leftrightarrow K_0$ and $\delta=\gamma^{-1}\leftrightarrow K_1$, it follows that $r(\gamma_{p/q})=\gamma_{-p/q}$ represents the same element as $\gamma_{p/q}$ in $\pi_1(\mathcal{S})$.

We will show that if $p'/q'\neq\pm p/q+2k$ for $k\in\mathbb{Z}$, then $\gamma_{p/q}\nsim\gamma_{p'/q'}$ after computing traces; see Corollary 4.13. □

4.4 Step 2: Computation of traces

Let $V_{p/q}\in \mathrm{SL}(2,\mathbb{C})=\rho_x(\gamma_{p/q})$, where, since we want to compute $\operatorname{Tr} V_{p/q}$, we only need to consider $V_{p/q}$ up to cyclic permutation and inversion, and hence $\gamma_{p/q}$ only up to free homotopy. Rather than using the associated torus tree, we will work directly with a 4–holed sphere $\Sigma_{0,4}$ and the associated tree as described in [22]; see also [9]. Let $\alpha,\beta,\gamma,\delta$ denote loops round the four holes, oriented so that $\alpha\beta\gamma\delta=\mathrm{id}$. The fundamental group is identified with the free group F_3 with generators α,β,γ. A representation $\rho\colon F_3\to\mathrm{SL}(2,\mathbb{C})$ is determined up to conjugation by its values on seven elements as follows (where we use $\widehat{w}$ in place of w in [22] etc to distinguish it from a variable w already in other use):

$$\operatorname{Tr}\rho(\alpha)=a;\quad \operatorname{Tr}\rho(\beta)=b;\quad \operatorname{Tr}\rho(\gamma)=c;\quad \operatorname{Tr}\rho(\delta)=d$$
$$\operatorname{Tr}\rho(\alpha\beta)=\hat{x};\quad \operatorname{Tr}\rho(\beta\gamma)=\hat{y};\quad \operatorname{Tr}\rho(\gamma\alpha)=\hat{z}$$

related by the equation

$$\hat{x}^2+\hat{y}^2+\hat{z}^2+\hat{x}\hat{y}\hat{z}=\hat{p}\hat{x}+\hat{q}\hat{y}+\hat{r}\hat{z}+\hat{s}, \tag{4-1}$$

where

$$\hat{p}=ab+cd,\quad \hat{q}=bc+ad,\quad \hat{r}=ac+bd,\quad \hat{s}=4-a^2-b^2-c^2-d^2-abcd.$$

We identify our generators K_i as: $\alpha\leftrightarrow K_0$, $\beta\leftrightarrow K_1$, $\gamma\leftrightarrow K_2$, $\delta\leftrightarrow K_3$. Thus we find

$$a=b=c=d=-1,\qquad \begin{aligned}\hat{x}&=\operatorname{Tr}K_0K_1=x,\\ \hat{y}&=\operatorname{Tr}K_1K_2=2,\\ \hat{z}&=\operatorname{Tr}K_2K_0=-x+1.\end{aligned}$$

As a check, it is easy to verify that the trace identity (4-1) holds. Notice that none of the expressions $\hat{p},\dots,\hat{z}$ depend on the sign choices made in Section 3.2.2.

The traces can be arranged in a trivalent tree in the usual way. As explained above, we have $\gamma_{0/1}\leftrightarrow K_0K_1$, $\gamma_{1/0}\leftrightarrow\mathrm{id}$, $\gamma_{1/1}\leftrightarrow K_0K_1^{-1}$. As explained in [22, Section 2.10], there are now 3 moves, depending on the values of $\hat{p},\hat{q},\hat{r}$. In our case, $\hat{p}=\hat{q}=\hat{r}=2$, so the three moves described there coincide. Following [22], if u,v,w are labels round a vertex, with v,w labels adjacent along a common edge e, then the label at the vertex at the opposite end of e is $u'=2-vw-u$; compare Figure 3 in which $u'=vw-u$.

Clearly this procedure gives an algorithm for arranging curves and computing traces on a trivalent tree by analogy with that described in Section 2. Curves generated in this way inherit a natural labelling from the usual procedure of Farey addition as described in Section 2. Denote the curve which inherits the label p/q by $\delta_{p/q}$; we say this curve is in *Farey position* p/q on the tree. We shall refer to this tree together with its new rule for computing traces as the $\mathcal{S}$–tree, to distinguish it from the Markoff tree of Section 2.

We need to show that $\delta_{p/q}$ is the same as the curve $\gamma_{p/q}$ described in the previous section, namely the curve with $2q$ intersections with the meridian ∂m and a twist by p.

Lemma 4.10 *With the above notation,* $\delta_{p/q} = \gamma_{p/q}$.

Proof By definition we have $\delta_{p/q} = \gamma_{p/q}$ for $p, q \in \{0, 1\}$. With the notation above, these are the curves $\alpha\beta, \beta\gamma, \gamma\alpha$, each of which separates the punctures in pairs.

Call two essential simple nonperipheral curves on $\partial\mathcal{S}$ *neighbours* if they intersect exactly twice when in minimal position. Note that of the initial triple, each pair adjacent along an initial edge are neighbours, so that the triple round the initial vertex are neighbours in pairs. Note also that given a pair of neighbours δ, δ', there are exactly two other curves which are neighbours of both δ and δ'. If δ, δ' are adjacent along an edge of the tree, then these two further curves are exactly the remaining curves adjacent to the vertices at the ends of e.

These two further curves can be found by surgery, more precisely, by the Luo product defined in [21]. This works as follows. Arrange δ, δ' so as to have minimal intersection, cut them at their two intersection points and then make a consistent choice of the direction in which to turn to rejoin the resulting arcs. The Luo product rejoins the arcs by turning left at each intersection point (relative to a fixed orientation on the surface) as illustrated in Figure 10; equally we could rejoin by turning right at both intersection points. We denote the resulting curves by $\delta \cdot_L \delta'$ and $\delta \cdot_R \delta'$, respectively. It is not hard to see that $\delta \cdot_L \delta'$ is a neighbour of both δ and δ' and likewise for $\delta \cdot_R \delta'$. In particular, it is easy to check that $\delta_{0/1} \cdot_L \delta_{1/0} = \delta_{1/1}$ and $\delta_{0/1} \cdot_R \delta_{1/0} = \delta_{-1/1}$.

Now we show inductively that $\delta_{p/q} = \gamma_{p/q}$. As noted above, this is true for the initial values $0/1, 1/0, 1/1$ and $-1/1$. Suppose that it is true for neighbours $p/q, r/s$ where $|ps - rq| = 1$. By induction we may assume that $\delta_{p/q}, \delta_{r/s}$ are neighbours, hence adjacent along an edge e of the tree. By the above discussion we know that the additional curves at the two vertices of e are exactly $\delta_{p/q} \cdot_L \delta_{r/s}$ and $\delta_{p/q} \cdot_R \delta_{r/s}$. Moreover, by the inductive hypothesis, one of these curves must be $\delta_{r-p/s-q} = \gamma_{p-r/q-s}$ (or $\gamma_{r-p/s-q}$). Thus it remains only to show that the other curve is $\gamma_{p+r/q+s}$.

On each B_i, arrange $\delta_{p/q} = \gamma_{p/q}$ and $\delta_{r/s} = \gamma_{r/s}$ symmetrically with respect to the front and back of $\mathcal{S}$ as described above, then join the strands in the usual way.

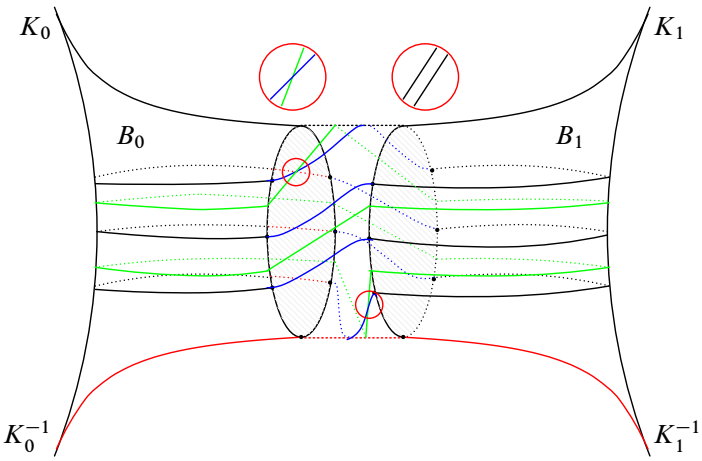

Figure 10: Here $\gamma_{1/3}$ and $\gamma_{1/2}$ are surgered to give $\gamma_{2/5}$; see the proof of Lemma 4.10. The inset circles show the direction of surgery.

With $\gamma_{p/q}$ in this position, its twist p is its intersection number with the geodesic α joining the two positive cone points given by the axes K_i, and likewise for $\gamma_{r/s}$. To take the Luo product, we have to cut $\gamma_{p/q}, \gamma_{r/s}$ at their intersection points and then make a consistent choice of which direction to rejoin the resulting arcs. Clearly the curve $\delta_{p/q} \cdot_L \delta_{r/s}$ with the "positive" surgery (see the inset circles in Figure 10) will have $2(q+s)$ intersection points with the meridian ∂m and intersection number $p+r$ with α, and hence must be $\gamma_{p+r/q+s}$. Since we already know the curve at one vertex of e is $\delta_{r-p/s-q} = \gamma_{p-r/q-s}$ (or $\gamma_{r-p/s-q}$), we must have $\delta_{p+r/q+s} = \gamma_{p+r/q+s}$. This completes the proof. □

In the following statement we make a particular, unimportant, choice of $\gamma_{p/q} \in \pi_1(\mathcal{S})$; see the beginning of Step 2 as above.

Proposition 4.11 *Let $V_{p/q}(x) = \rho_{\mathcal{S}}(x)(\gamma_{p/q})$. Then:*

(1) $\operatorname{Tr} V_{p/q} = \operatorname{Tr} V_{(p/q)+2} = \operatorname{Tr} V_{-p/q}$.

(2) $\operatorname{Tr} V_{p/q}(x) = \operatorname{Tr} V_{(p+q)/q}(1-x)$.

(3) $\operatorname{Tr} V_{p/q}$ *is a polynomial in* x. *If* $0 \le p/q \le 1$, *then its top two terms are* $(-1)^{p-q-1}(x^q - px^{q-1})$.

Remark 4.12 (3) should be compared to [15, Corollary 4.3] in which we showed that the leading term is of the form $(-1)^{p-q-1}cx^q$ for some $c > 0$; see also the remark following the corollary in that paper. Notice that by (1) and (2), it suffices to find the traces of curves the interval $0 \le p/q \le 1$.

Proof (1) This follows immediately from Proposition 4.9 and can also be proved easily by looking at the symmetries of the $\mathcal{S}$–tree.

(2) This results from the symmetry $x \mapsto 1-x$ which interchanges $\gamma_{0/1}, \gamma_{1/1}$.

(3) Note (1) holds for the three initial traces of $\gamma_{0/1}, \gamma_{1/0}, \gamma_{1/1}$. If curves $\gamma_{p/q}, \gamma_{r/s}$ are adjacent along an edge, then the two curves at the remaining vertices at the ends of the edge are $\gamma_{p\pm r/q\pm s}$. The result then follows easily by induction on the tree. □

Now we can prove the "only if" assertion of Proposition 4.9:

Corollary 4.13 *If $p'/q' \neq \pm p/q + 2k$ for $k \in \mathbb{Z}$, then $\gamma_{p/q} \not\sim \gamma_{p'/q'}$.*

Proof This follows directly by comparing the top two terms of $\operatorname{Tr} V_{p/q}, \operatorname{Tr} V_{p'/q'}$. □

4.5 Step 3: The exceptional Fuchsian case: computation of $\mathcal{P}_{0/1}$, $\mathcal{P}_{1/1}$

As above, let $\mathcal{P}_{p/q}$ denote the pleating ray of $\gamma_{p/q}$. The rays $\mathcal{P}_{0/1}, \mathcal{P}_{1/1}$ are exceptional. Since $\gamma_{0/1} \leftrightarrow K_0K_1$, $\gamma_{1/1} \leftrightarrow K_0K_1^{-1}$, we have $\operatorname{Tr} V_{0/1} = x$, $\operatorname{Tr} V_{1/1} = 1-x$. Thus the real locus for both trace polynomials is exactly the real axis, and on this locus, the group $G_{\mathcal{S}}(x)$, if discrete, is Fuchsian. This is exactly the situation discussed in [15, page 84].

In the ball model of $\mathbb{H}^3$, identify the extended real axis with the equatorial circle. Since the limit set is contained in $\widehat{\mathbb{R}}$, the convex core (the Nielsen region) of $G_{\mathcal{S}}(x)$ is contained in the equatorial plane. We can think that the convex core has been squashed flat and the bending lines are just the boundary of the Nielsen region, that is, the boundary of the convex core of the surface $\mathbb{H}^2/G_{\mathcal{S}}(x)$. Thus to find the bending lamination we just have to determine the boundary of $\mathbb{H}^2/G_{\mathcal{S}}(x)$.

Now if $x \in \mathbb{R}$, then either $\zeta \in \mathbb{R}$ and $x > 0$, or $\zeta \in i\mathbb{R}$ and $x < 0$. In both cases, we find a fundamental domain for $G_{\mathcal{S}}(x)$ as described in Section 4.1; see Figure 11. Thus regarded as a Fuchsian group acting on the upper half plane $\mathbb{H}$, $G_{\mathcal{S}}(x)$ represents a sphere with two order-3 cone points and one hole. However the cases $x < 0$ and $x > 0$ are slightly different, because of the relative directions of rotation of K_0 and K_1.

In both cases, the axis K_0 has fixed points $\pm i\sqrt{3}$ and its axis is oriented so that it is anticlockwise rotation about $i\sqrt{3}$. Thus $K_1 = PK_0P^{-1}$ rotates anticlockwise about $P(i\sqrt{3}) = -i\zeta^2/\sqrt{3}$. If $x < 0$ then $P(i\sqrt{3})$ is in the upper half plane $\mathbb{H}$, while if $x > 0$ then $P(i\sqrt{3})$ is in the lower half plane. Hence if $x < 0$ then K_0, K_1 rotate in the same sense about their fixed points in $\mathbb{H}$, while if $x > 0$ their rotation directions are opposite. This leads to the two different configurations shown in Figure 11.

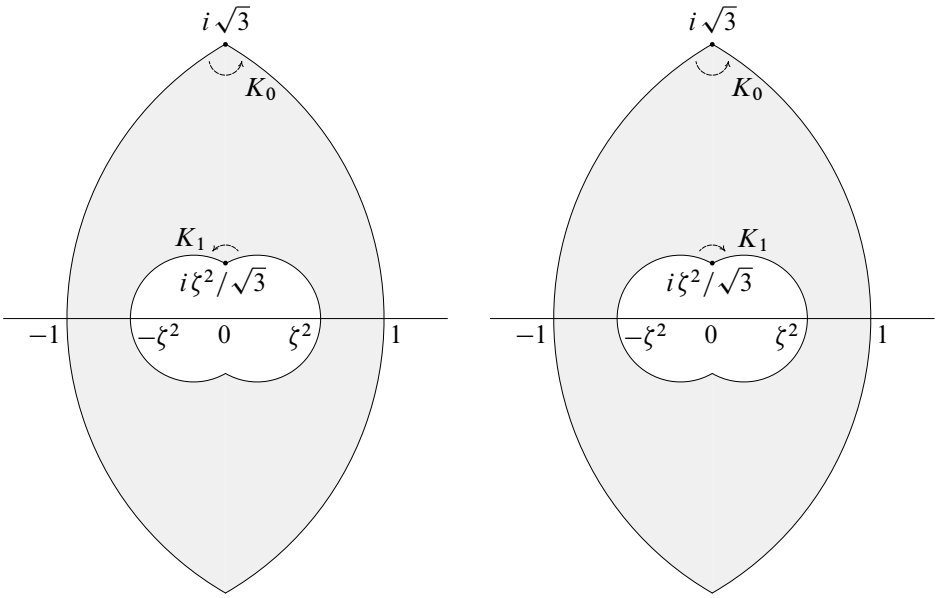

Figure 11: Configurations for $x \in \mathbb{R}$. Left: $\zeta \in i\mathbb{R}$, $x \leq -2$; K_0 and K_1 rotate in the same directions $\mathbb{H}$ and the hole is K_0K_1. Right: $\zeta \in \mathbb{R}$, $x \geq 3$; K_0 and K_1 rotate in opposite directions in $\mathbb{H}$ and the hole is $K_0K_1^{-1}$.

As is easily checked, if $x > 0$ the boundary of the hole is thus $K_0K_1^{-1}$ while if $x < 0$ the boundary of the hole is K_0K_1. Since $K_0K_1 \leftrightarrow \gamma_{0/1}$ and $K_0K_1^{-1} \leftrightarrow \gamma_{1/1}$, combining this with information about the discreteness locus in the Fuchsian case from Section 4.1, we conclude that $\mathcal{P}_{0/1} = (-\infty, -2]$ and $\mathcal{P}_{1/1} = [3, \infty)$.

4.6 Step 4: Nonsingularity of pleating rays

This is the part of the argument which contains the deepest mathematics. Fortunately, the results needed have been proved elsewhere.

Theorem 4.14 [18; 15; 5] *Suppose that $\gamma \in \pi_1(\mathcal{S})$. Then $\mathcal{P}_\gamma$ is open and closed in the real trace locus $\mathbb{R}_\gamma$. Moreover, $\operatorname{Tr}\rho_x(\gamma)$ is a local coordinate for $\mathbb{C}$ in a neighbourhood of $\mathcal{P}_\gamma$, and is a global coordinate for $\mathcal{P}_\gamma$ on any nonempty connected component of $\mathcal{P}_\gamma$.*

Proof The statement that $\mathcal{P}_\gamma$ is open in $\mathbb{R}_\gamma$ is essentially [15, Proposition 3.1]; see also [18, Theorems 15 and 26]. The fact that $\operatorname{Tr}\rho_x(\gamma)$ is a local parameter is equivalent to the fact, also proved in both [15] and [14], that $\mathcal{P}_\gamma$ is a nonsingular 1–manifold. The openness and the final statement are actually a special case of Theorems B and C

of [5] which state that for general hyperbolic manifolds, if the support of the bending lamination is rational (a union of closed curves), then the traces of these curves are local parameters for the deformation space in a neighbourhood of the corresponding pleating variety.

That $\mathcal{P}_\gamma$ is closed in $\mathbb{R}_\gamma$ can be proved as in [15, Theorem 3.7]. Here is a slightly more sophisticated version of the same idea. Suppose $x_n \to x_\infty$ with $x_n \in \mathcal{P}_\gamma$. The limit group $G_S(x_\infty)$ is an algebraic limit of groups $G_S(x_n)$ and hence the corresponding representation is discrete and faithful. Each of the two components of $(\partial\mathcal{C}/G_S(x_n))\setminus\gamma$ is a flat surface corresponding to a conjugacy class of Fuchsian subgroup $F_j(x_n)$ for $j = 1, 2$ (the F–peripheral subgroups of [15]). Since the limit is algebraic, $F_j(x_n)$ limits on a Fuchsian subgroup $F_j(x_\infty)$, and similarly for all its conjugates in $G_S(x_\infty)$.

The limit sets Λ_α of each of these subgroups F_α is spanned by a hyperbolic plane H_α in $\mathbb{H}^3$. The Nielsen regions of F_α in H_α fit together along the lifts of the bending line γ to $\mathbb{H}^3$, forming a pleated surface Π in $\mathbb{H}^3$. We claim that $\Pi = \partial\mathcal{C}(G_S(x_\infty))$. This follows since the closure of the union of the Λ_α is the limit set of $G_S(x_\infty)$; see also Proposition 7.2 in [17]. The result follows. □

Remark 4.15 The closedness of $\mathcal{P}_\gamma$ in $\mathbb{R}_\gamma$ is a simple case of both the "local limit theorem", Theorem 15 in [18] and the "lemme de fermeture" of [2]. These much more sophisticated results allow that the bending lines may be part of an irrational lamination. Our argument above, in which the bending lamination is supported on closed curves, is very close to that in the first part of the proof of Théorème 6 in [26].

Corollary 4.16 [14; 15; 5] *If $\mathcal{P}_\gamma \neq \varnothing$, then it is a union of connected nonsingular branches of the real trace locus $\mathbb{R}_\gamma$.*

Proof Suppose that $\mathcal{P}_\gamma \neq \varnothing$ and let $x \in \mathcal{P}_\gamma$, so that by Lemma 4.6, $x \in \mathbb{R}_\gamma$. By Theorem 4.14, $\mathcal{P}_\gamma$ is open and closed in $\mathbb{R}_\gamma$. Since $\operatorname{Tr}\rho_x(\gamma)$ is a local coordinate, in a neighbourhood of x the locus $\mathbb{R}_\gamma$ is a 1–manifold. □

Notice that the theorem says that $\operatorname{Tr}\rho_x(\gamma)$ is a local parameter even in a neighbourhood of a cusp where $\rho_x(\gamma)$ is parabolic [5, Theorem C]. Thus we have

Corollary 4.17 *Suppose that $x \in \mathcal{P}_\gamma$. Then there is a neighbourhood of x in $\mathbb{C}$ on which $x \in \mathbb{R}_\gamma$ implies that $x \in \mathcal{D}$.*

Corollary 4.18 *If $\mathcal{P}_\gamma \neq \varnothing$, then $\operatorname{Tr}\rho_x(\gamma)$ is unbounded on $\mathcal{P}_\gamma$.*

Proof Since $\operatorname{Tr}\rho_x(\gamma)$ is a local coordinate on connected components of $\mathcal{P}_\gamma$, this follows from the maximum principle on the branch; see [15, Theorem 4.1]. □

4.7 Step 5: Finding the nonempty pleating rays

Now we determine the pleating rays. As above, let $\mathcal{P}_{p/q}$ denote the ray corresponding to the curve $\gamma_{p/q}$ and write $\mathbb{R}_{p/q}$ for the real locus of $\operatorname{Tr} V_{p/q}$. From Proposition 4.9 we have $\mathcal{P}_{p/q} = \mathcal{P}_{(p+2q)/q} = \mathcal{P}_{-p/q}$.

By Section 4.6, $\mathcal{P}_{p/q}$ is a union of nonsingular branches of $\mathbb{R}_{p/q}$. We now find those $p/q \notin \{0, 1\}$ for which $\mathcal{P}_{p/q} \neq \varnothing$, at the same time resolving the connectivity issue. We follow the method of [15], using an inductive argument on position of the pleating rays and their asymptotic directions as $|x| \to \infty$, and at the same time correcting the second of the two errors referred to in Remark 4.7. We have:

Proposition 4.19 (cf [15, Theorem 4.1]) *The set $\mathcal{P}_{p/q}$ is the union of the two branches of $\mathbb{R}_{p/q}$ which are asymptotic to the half lines $\rho e^{\pm i\pi(p-q)/q}$ as $\rho \to \infty$.*

Proof Denote by $R(\theta)$ the ray $te^{i\theta}, t > 0$, in the x–plane. By Proposition 4.11, $\operatorname{Tr} V_{p/q}$ is a polynomial in x whose top term is $(-1)^{p-q-1}x^q$. Now $\operatorname{Tr} V_{p/q}$ takes real values on $\mathcal{P}_{p/q}$, moreover by Corollary 4.18 it is unbounded on $\mathcal{P}_{p/q}$. It follows that $\mathcal{P}_{p/q}$ must be asymptotic to one of the rays $R(k\pi/q)$ for some $k \in \mathbb{Z}$ as $|x| \to \infty$.

We have already identified $\mathcal{P}_{0/1}$ and $\mathcal{P}_{1/1}$ as the real intervals $(-\infty, -3]$ and $[2, \infty)$, respectively. It follows from Section 4.1 that the semicircular arc from -4 to 4 (say) in $\mathbb{H}$ is a continuous path in $\mathcal{D}$ from $\mathcal{P}_{0/1}$ to $\mathcal{P}_{1/1}$. Hence by the continuity theorem of [16], if $0 < p/q < 1$, there is a point on $\mathcal{P}_{p/q}$ in the upper half plane $\mathbb{H}$. Likewise, there is a point on $\mathcal{P}_{p/q}$ in the lower half plane. (This was missed in [15].) Since $\mathcal{P}_{0/1} \cup \mathcal{P}_{1/1}$ separates $\mathcal{D}$ into two connected components, this shows in particular that $\mathcal{P}_{p/q}$ must have at least two connected components.

Now we proceed by induction on the Farey tree. Suppose we have shown the result for two Farey neighbours $p/q, r/s$. Consider the locus $\mathcal{P}_{p+r/q+s}$. By the inductive hypothesis, $\mathbb{H}$ contains exactly one component of each of $\mathcal{P}_{p/q}, \mathcal{P}_{r/s}$, asymptotic to the rays $R(\pi(p-q)/q), R(\pi(r-s)/s)$, respectively. Exactly as in [15], it is easy to check that there is exactly one integer $k \in \{0, 1, \dots, 2(q+s)-1\}$ for which $R(k\pi/(q+s))$ lies between $R(\pi(p-q)/q)$ and $R(\pi(r-s)/s)$, namely $k = (p+r)/(q+s)$. By the same continuity theorem as before, a path in this sector joining suitable points on $\mathcal{P}_{p/q}, \mathcal{P}_{r/s}$ must meet $\mathcal{P}_{p+r/q+s}$. Thus $\mathcal{P}_{p+r/q+s}$ has at least one connected component asymptotic to $R(\pi(p+r-q-s)/(q+s))$. A similar argument in the lower half plane gives another connected component asymptotic to $R(\pi(p+r+q+s)/(q+s))$. Since $\mathcal{P}_{p+r/q+s}$ has exactly two components by Proposition 4.20 below, the result follows. □

The issue of connectivity of $\mathcal{P}_\gamma$ is a bit subtle. In the general theory (see [2; 5]), one shows that $\mathcal{P}_\gamma$ has one connected component. However this result holds in a space

of manifolds which are consistently oriented throughout the space and all of whose convex cores have nonzero volume. In our case we have:

Proposition 4.20 *If $\gamma \neq \gamma_{0/1}, \gamma_{1/1}$ and $\mathcal{P}_\gamma \neq \varnothing$, then $\mathcal{P}_\gamma$ has exactly two connected components in $\mathcal{D}$.*

Proof The usual argument that the pleating ray of a rational lamination has one connected component goes as follows. Given a point on $\mathcal{P}_\gamma$, double the convex core along its boundary to obtain a cone manifold with a singular axis of angle $2(\pi-\theta)$ along γ, where θ is the bending angle along γ. (Notice that the convention on defining bending angles differs between papers by the first author and [2]. In our convention, a bending line contained in flat subsurface has bending angle 0 but cone angle 2π, whereas in [2], the bending angle along a line in a flat surface is defined to be π.) By [13], such a hyperbolic cone manifold is parametrised by its cone angle. One shows that one can continuously deform the cone angle to 0, at which point the curve whose axis is the bending line has to become parabolic. The doubled manifold is an oriented hyperbolic manifold with a rank-two cusp and finite volume. As long as we are working in a space in which all manifolds have consistent orientation, such a manifold is unique up to orientation-preserving isometry, from which one deduces that $\mathcal{P}_\gamma$ is connected.

In our case, the parameter space $\mathcal{D}$ is separated by two lines along which G is Fuchsian so that $\mathcal{C}(G)/G$ has zero volume and the above argument fails. Note however that, provided that G is not Fuchsian, $\mathcal{S}$ can be oriented by the triple consisting of the *oriented* axes of P, Q and the oriented line C from $\operatorname{Ax} K_0$ to $\operatorname{Ax} K_1$. The map $\zeta \to \overline{\zeta}$ reverses the relative orientations of $\operatorname{Ax} P, \operatorname{Ax} Q$ while fixing that of C. Thus $\mathcal{D} \setminus \mathbb{R}$ has two connected components in which $\mathcal{S}$ has naturally opposite orientations. The above argument shows that $\mathcal{P}_\gamma$ has at most one component in each component of $\mathcal{D}$. Since we have already shown in Proposition 4.19 that $\mathcal{P}_\gamma$ has at least one component in each of the upper and lower half planes, this completes the proof.

This result can alternatively be proved by the more ad hoc methods used in [15]. □

Remark 4.21 Proposition 4.19 shows that $\mathcal{P}_{p/q} \neq \varnothing$ for all $p/q \in \mathbb{Q}$. This can be viewed as a special case of the general result of [2, Theorem 1]; see also [5, Theorem 2.4]. We have to be careful to include the case, excluded in [2], that the group $G_{\mathcal{S}}(x)$ is Fuchsian so that $\mathcal{C}/G$ has zero volume. The conclusion is the following:

Proposition 4.22 *Let γ be an essential simple nonperipheral closed curve on $\partial\mathcal{S}$. Then $\mathcal{P}_\gamma \neq \varnothing$ if and only if γ is nontrivial in $\pi_1(\mathcal{S})$ and intersects the meridian disk $\gamma_{1/0}$ at least twice. If γ meets $\gamma_{1/0}$ exactly twice, then the bending angle is identically π and $G_{\mathcal{S}}(x)$ is Fuchsian.*

4.8 Step 6: Density of rational pleating rays

Finally, we justify the claim that the rational pleating rays are dense in $\mathcal{D}$:

Theorem 4.23 [14, Corollary 6.2; 15, Theorem 5.2] *Rational pleating rays are dense in $\mathcal{D}_\mathcal{S}$.*

Proof The proof of this result in any one-complex-dimensional parameter space is the same. Here is a quick sketch. Suppose that ν is an irrational lamination with corresponding pleating variety $\mathcal{P}_\nu$, and that $x \in \mathcal{P}_\nu$. Pick a sequence of rational measured laminations $\nu_n = c_n\delta_{\gamma_n}$ where $c_n \in \mathbb{R}^+$ so that $\nu_n \to \nu$ in the space of projective measured laminations on $\partial\mathcal{S}$, where δ_{γ_n} is the unit point mass on γ_n. Replace the traces of γ_n by complex length functions λ_n and scale to get complex analytic functions $c_n\lambda_n$. One shows that in a neighbourhood of $x \in \mathcal{P}_\nu$ these functions form a normal family which converges to a nonconstant analytic function [14, Theorem 6.9; 18, Theorem 20], whose real locus contains the pleating ray $\mathcal{P}_\nu$ [18, Theorem 23]. By Hurwitz's theorem, there are nearby points at which the approximating functions $c_n\lambda_n$ must take on real values. In a small enough neighbourhood of x, this is enough to force $y \in \mathcal{P}_{\gamma_n}$ [18, Theorem 31]. This gives density in $\operatorname{Int}\mathcal{D}$. By the result quoted in the introduction that $\mathcal{D} = \overline{\operatorname{Int}\mathcal{D}}$ we are done. □

Remark 4.24 $\mathcal{D}$ as defined above (see the beginning of Section 4) includes the parabolic cusp groups on $\partial\mathcal{D}$. In fact these groups are exactly the geometrically finite groups on $\partial\mathcal{D}$, and hence exactly the groups in $\mathcal{D}$ but not in $\mathcal{SCH}$ as defined in the introduction. Since there are only countably many such groups, and since $\operatorname{Int}\mathcal{D} = \mathcal{SCH}$, whether or not we include them in the parameter space does not materially affect our computations. See [23] for more on this and related issues.

4.9 The pleating rays for $\mathcal{H}$

By Corollary 4.3, $\mathcal{D}_\mathcal{H} = \mathcal{D}_\mathcal{S}$. Thus the rational rays for $\mathcal{D}_\mathcal{S}$ are also dense in $\mathcal{D}_\mathcal{H}$. However it is easy to see that a rational pleating laminations on $\partial\mathcal{H}(x)$ correspond exactly to those on $\mathcal{S}(x)$, and that although the actual bending curves differ, their traces are related by a simple formula.

Lemma 4.25 *Suppose that the bending lamination $\beta_\mathcal{H}(x)$ of $\mathcal{H}(x)$ is rational, so that its support λ is a union of disjoint simple closed curves on $\partial\mathcal{H}$. Let γ be a connected component of λ. Then either $\kappa(\gamma) = \gamma$ or the three curves $\gamma, \kappa(\gamma), \kappa^2(\gamma)$ are disjoint. The support of the bending lamination $\beta_\mathcal{S}(x)$ is exactly the projection of γ to $\mathcal{S}$, and all rational bending laminations of $\mathcal{S}$ arise in this way.*

Proof The limit set of $G_{\mathcal{H}}(x)$ and hence its convex core are invariant under the symmetry κ. Hence the support λ of $\beta_{\mathcal{H}}(x)$ is also κ–invariant. Let γ be a connected component of λ. Since connected components of λ are pairwise disjoint, either $\kappa(\gamma) = \gamma$ or the three curves $\gamma, \kappa(\gamma), \kappa^2(\gamma)$ are disjoint. In either case, γ cannot pass through a fixed point of κ: at the fixed point P the images of γ would meet at angles $\frac{2\pi}{3}$, so that $\gamma, \kappa(\gamma), \kappa^2(\gamma)$ would intersect at P, which is impossible.

Let π_κ be the projection $\mathcal{H} \to \mathcal{S}$. In a neighbourhood of a bending line π_κ is a covering map hence a local isometry. Since being a bending line can be characterised locally, $\beta_{\mathcal{S}}(x)$ is the projection of γ to $\mathcal{S}$.

Let γ be a simple closed curve on $\partial\mathcal{S}$. Clearly, by the same observation about local characterisation of bending lines, if γ is a bending line, then so is any connected component of its lift to $\partial\mathcal{H}$. This proves the converse. □

We remark that if p/q is congruent to $1/0$ or $0/1$ mod $\mathbb{Z}_2$, then the lift of $\gamma_{p/q}$ has three connected components which are permuted among themselves by κ, while if p/q is congruent to $1/1$, then its lift has one κ–invariant connected component. To see this, check by hand for the curves $\gamma_{1/0}, \gamma_{0/1}, \gamma_{1/1}$ and then note that the lifting property is invariant under the mapping class group of $\partial\mathcal{S}$ which at the same time acts transitively on p/q congruence classes mod $\mathbb{Z}_2$.

To actually compute the pleating rays for $\mathcal{D}_{\mathcal{S}}$, we computed the traces $\operatorname{Tr} V_{p/q}(x)$ corresponding to the curves $\gamma_{p/q} \in \pi_1(\mathcal{S})$. The above discussion shows that it is unnecessary to actually compute traces of lifted curves in $\pi_1(\mathcal{H})$. If for some reason one wanted to do this, either one could start again enumerating the curves on $\mathcal{H}$, or one could note that the complex length of a lift of $\gamma_{p/q}$ in $\mathcal{H}$ would be either the same as or three times that of the curve $\gamma_{p/q}$ in $\mathcal{S}$, depending on the $\mathbb{Z}_2$–parity of p/q.

5 Computing traces

To compute traces of the elements $V_{p/q}$, rather than use the $\mathcal{S}$–tree as in Section 4.4, we actually performed computations on the associated Markoff tree corresponding to the associated torus $\mathcal{T}$ of Section 3.2.3, referred to in this section as the $\mathcal{T}$–tree. To justify this, we need to compare the curves in Farey position p/q on the two trees to ensure that they do indeed correspond geometrically as expected. We also need to address the issue about lifting representations to $\mathrm{SL}(2,\mathbb{C})$ raised in Remark 3.2.

5.0.1 Correspondence of curves Homotopy classes of essential simple nonperipheral loops on $\partial\mathcal{T}$ are well known to be in bijective correspondence to unoriented lines

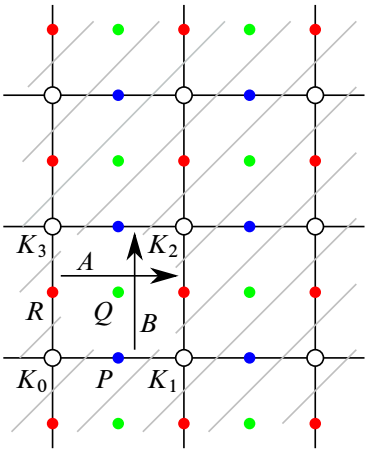

Figure 12: Lattice representation of a cover of $\partial\mathcal{S}$. The integer vertices (open circles) correspond to the endpoints of the order-3 axes on $\partial\mathcal{S}$; the endpoints of the order-2 elliptics P, Q and R are on horizontal segments (blue), in the middle of squares (green), and on vertical segments (red), respectively.

of rational slope in the plane; see for example [27; 14]. In fact the word $W_{p/q}$ generated by the concatenation process following the $\mathcal{T}$–tree described in Section 2 is the cutting sequence of a line of slope $p/q \in \hat{\mathbb{Q}}$ across the lattice; see [27].

The key point here is that the plane with a cone singularity of angle $\frac{4\pi}{3}$ at integer lattice points (see Figure 12), is an intermediate covering between the universal cover $\mathbb{H}$ of $\partial\mathcal{T}$ and $\partial\mathcal{T}$ itself. As described in for example [15], the same lattice can also be viewed as an intermediate covering between $\mathbb{H}$ and $\partial\mathcal{S}$: the rectangle with vertices at $0, 1, 2i, 2i+1$ can be viewed as a fundamental domain for the lattice action corresponding to $\partial\mathcal{S}$ which projects, bijectively on its interior, to $\partial\mathcal{S}$. Likewise, the rectangle with vertices $0, 1, \frac{1}{2}i, 1+\frac{1}{2}i$ projects in a similar way to $\partial\mathcal{U}$ and the unit square projects to the torus $\partial\mathcal{T}$. The lattice points correspond to the cone points belonging to K_i for $i = 1, \dots, 4$ arranged as shown. Thus there is also a bijective correspondence between lines of rational slope in the punctured plane and simple essential nonperipheral curves on $\partial\mathcal{S}$. In this way, one can easily relate the words $W_{p/q}$ (on $\partial\mathcal{T}$) and $V_{p/q}$ (on $\partial\mathcal{S}$); this is explained in detail in [15].

In this picture, the meridian loop ∂m of Section 4.3 is identified as the "vertical" line of slope $1/0$. One sees easily that the line of slope p/q in the plane projects to a curve on $\partial\mathcal{S}$ which has exactly $2q$ intersections with ∂m and a twist of p as described in Section 4.3. It follows from Lemma 4.10 that the labelling of curves by lines of rational slope p/q exactly corresponds to the Farey labelling of curves by their position on the $\mathcal{S}$–tree.

As above, the curve represented in Farey position p/q on the $\mathcal{S}$–tree is denoted by $\gamma_{p/q}$, corresponding to the word $V_{p/q}$; while the curve represented in Farey position p/q on the $\mathcal{T}$–tree is denoted by $\omega_{p/q}$, corresponding to the word $W_{p/q}$. Now $\mathcal{S}$ projects to $\mathcal{U}$ by a four-fold cover and $\mathcal{T}$ projects to $\mathcal{U}$ by a two-fold cover.

Proposition 5.1 *The complex translation length of the geodesic representative of $\gamma_{p/q}$ is twice that of $\omega_{p/q}$; hence* $\operatorname{Tr} V_{p/q}(\zeta) = \pm((\operatorname{Tr} W_{p/q}(\zeta))^2 - 2)$.

Note that this allows for an ambiguity in the signs of the traces since the two lifts of $\pi_1(\mathcal{T})$ and $\pi_1(\mathcal{S})$ to $\mathrm{SL}(2,\mathbb{C})$ are not (indeed cannot be) chosen consistently.

Corollary 5.2 *Up to sign, the trace of the image $V_{p/q}$ of $\gamma_{p/q} \in \pi_1(\mathcal{U})$ may be computed using the formula of Proposition 5.1 and the $\mathcal{T}$–tree.*

Since we are aiming to compute pleating rays which are a geometrical construct and hence only depend on a $\mathrm{PSL}(2,\mathbb{C})$ representation, this would be sufficient for our purposes. However it is more satisfying to prove the following more precise result which shows that working with the $\mathrm{SL}(2,\mathbb{C})$ lift of the representation of $\pi_1(\mathcal{T})$ described in Section 3.2.3, we can fix the choice of sign.

Proposition 5.3 *With $W_{p/q}, V_{p/q}$ as above, let $f_{p/q}(\zeta) = \operatorname{Tr} V_{p/q}(\zeta)$ and $g_{p/q}(\zeta) = \operatorname{Tr} W_{p/q}(\zeta)$. Then $-f_{p/q}(\zeta) = (g_{p/q}(\zeta))^2 - 2$ for all $p/q \in \widehat{\mathbb{Q}}$.*

Proof It is easy to check that this is correct for $p/q = 0/1, 1/0, 1/1$. In detail, (recalling that as above $\gamma \leftrightarrow Z$ means that $\gamma \in \pi_1(\mathcal{S})$ or $\pi_1(\mathcal{T})$ is represented by $Z \in \mathrm{SL}(2,\mathbb{C})$):

- $\omega_{0/1} \leftrightarrow A$ and $\gamma_{0/1} \leftrightarrow K_0K_1$, and we have shown that $A^2 = -K_0K_1$. Thus $f_{0/1}(\zeta) = x$ and $(g_{0/1}(\zeta))^2 - 2 = (-x+2) - 2 = -x$.
- $\omega_{1/0} \leftrightarrow B$, $\gamma_{1/0} \leftrightarrow \mathrm{id}$ and $B^2 = -\mathrm{id}$. So $f_{1/0}(\zeta) = 2$ and $(g_{1/0}(\zeta))^2 - 2 = -2$.
- $\omega_{1/1} \leftrightarrow AB$ and $\gamma_{1/1} \leftrightarrow K_0K_1^{-1}$. So $f_{1/1}(\zeta) = 1-x$ and $(g_{1/1}(\zeta))^2 - 2 = x-1$.

Now we do an inductive proof. Suppose that in the $\mathcal{S}$–tree labels u, v are adjacent along an edge e with w the remaining label at one of the two vertices at the ends of e. By the formula in Section 4.4 the label at the other vertex is $2 - uv - w$.

Suppose that the corresponding labels on the $\mathcal{T}$–tree are u', v', w'. Then the remaining label at the vertex at the other end of e is $u'v' - w'$. Replace these labels by the negatives of the traces of the doubled curves to get labels $2-u'^2, 2-v'^2, 2-w'^2, 2-(u'v'-w')^2$ around the same 4 vertices. If we can show that

$$2 - (2-u'^2)(2-v'^2) - (2-w'^2) = 2 - (u'v' - w')^2,$$

we will be done. This is easily checked by multiplying out, noting that the trace identity (4-1) round a vertex of the $\mathcal{T}$–tree gives

$$u'^2 + v'^2 + w'^2 = u'v'w' + \operatorname{Tr}[A, B] + 2 = u'v'w' + 3. \qquad \square$$

5.0.2 The actual computations The above discussion justifies the method we actually used to perform computations involving traces on $\mathcal{S}$. Instead of computing on the $\mathcal{S}$–tree with initial traces $\operatorname{Tr}\rho_{\mathcal{S}}(\gamma_{0/1}) = \operatorname{Tr} K_0K_1 = x$, $\operatorname{Tr}\rho_{\mathcal{S}}(\gamma_{1/0}) = \operatorname{Tr}\mathrm{id} = 2$, $\operatorname{Tr}\rho_{\mathcal{S}}(\gamma_{1/1}) = \operatorname{Tr} K_0K_1^{-1} = 1 - x$, we used the $\mathcal{T}$–tree with initial triple $\operatorname{Tr} A = \pm i(3/(2\zeta) - \zeta/2)$, $\operatorname{Tr} B = 0$ and $\operatorname{Tr} AB = \pm(3/(2\zeta) + \zeta/2)$ corresponding to the generators A, B of $G_{\mathcal{T}}$. As in Section 3.2.3, $A^2 = -K_0K_1$, so that $\operatorname{Tr} A^2 = -x$. Since $\operatorname{Tr} B = 0$, we can find $\operatorname{Tr} AB$ from the identity $(\operatorname{Tr} A)^2 + (\operatorname{Tr} AB)^2 = \operatorname{Tr}[A, B] + 2 = 3$. Thus setting $(a, b, c) = (\operatorname{Tr} A, \operatorname{Tr} B, \operatorname{Tr} AB)$ we have

$$a^2 - 2 = -x, \quad c^2 = 1 + x.$$

It is easily checked that this is in accord with (3-2). Thus associated to $G_{\mathcal{T}}(x)$ we have the torus tree $(a, b, c) = (\sqrt{-x+2}, 0, \sqrt{x+1})$. This is the method we actually used to compute the pleating rays shown in Figure 1.

Remark 5.4 The sign of the square roots in the above can be uniquely determined by the formulae for traces in terms of ζ. What we actually did was to make an arbitrary choice and plot rays corresponding to curves in the range $0 \le p/q \le 1$, thus making a picture in the upper half plane which we could then reflect. As can be seen from Figure 4, the signs of the square roots in fact alternate periodically with period 4 rather than period 2, so that, for example, $\operatorname{Tr}\rho_{\mathcal{T}}(\gamma_3) = -\operatorname{Tr}\rho_{\mathcal{T}}(\gamma_1)$.

5.0.3 Computations for the Riley slice The traces needed to find the pleating rays for the Riley slice in the lower frame of Figure 8 were computed by a method similar to that described above. Our parameter x can be related to the parameter ρ of [15] by comparing the traces of the word in Farey position $0/1$: these are K_0K_1 in our case and XY in the notation of [15]. Thus we find that x corresponds to $\rho + 2$. For the Riley group a similar computation to the one above with $\operatorname{Tr}[A, B] = -2$ gives immediately $(\operatorname{Tr} A)^2 = -(\rho + 2)$ and $(\operatorname{Tr} AB)^2 = \rho + 2$. Thus writing in terms of the x–coordinate we find the initial triple $(\sqrt{-x}, 0, \sqrt{x})$.

5.0.4 Comparison of Bowditch sets It is interesting to compare the Bowditch sets associated to the two initial triples (x, x, x) and $(\sqrt{-x+2}, 0, \sqrt{x+1})$. In the latter case, one needs to modify the definition of the Bowditch set: since $\phi(U) = 0$ for some $U \in \Omega$, there is a trace-preserving $\mathbb{Z}$–action on the associated tree $\mathbb{T}_{(\sqrt{-x+2}, 0, \sqrt{x+1})}$ corresponding to the action of a subgroup of $\operatorname{Aut}(F_2)$ generated by a parabolic; see,

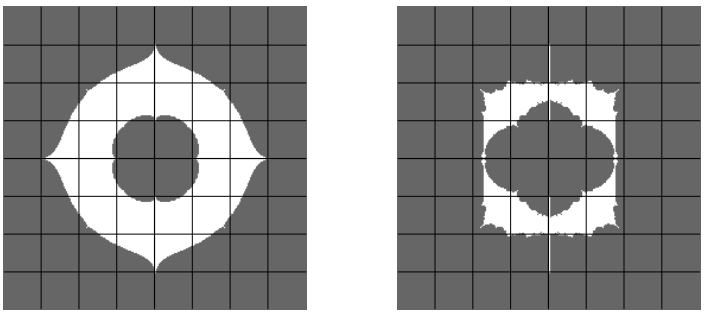

Figure 13: Bowditch sets (grey) plotted in the ζ–plane with range $[-4,4]\times[-4i,4i]$. Left: initial triple $(\sqrt{-x+2},0,\sqrt{x+1})$ corresponding to the torus group $G_{\mathcal{T}}(x)$. Right: initial triple (x,x,x) corresponding to the handlebody group $G_{\mathcal{H}}(x)$. The two regions are clearly distinct: the grey region on the right contains that on the left.

for example, [29, Theorem 1.6]. The Bowditch condition should actually be specified on $\Omega\setminus\{U\}/\sim$, where $\sim$ is the equivalence coming from this symmetry.

The results, plotted in the ζ–plane, are shown in Figure 13. On the right, the initial triple is (x,x,x) (with x related to ζ as in (3-1)) corresponding to the handlebody group $G_{\mathcal{H}}(x)$. On the left, the initial triple is $(\sqrt{-x+2},0,\sqrt{x+1})$ corresponding to the torus group $G_{\mathcal{T}}(x)$. The two regions are clearly distinct: the grey region on the right contains that on the left. Conjecturally, the left-hand grey region is also the discreteness locus for the groups $G_{\mathcal{T}}(x)$; see Figure 8 for the parametrisation in terms of x.

Note the various symmetries as discussed in Section 3.2.6, in particular note how Figure 5 looses the left-right reflectional symmetry seen in Figure 13. The coloured region in Figure 5 is the same region as the right frame of Figure 13, drawn in the x–plane.

References

[1] **H Akiyoshi**, **M Sakuma**, **M Wada**, **Y Yamashita**, *Punctured torus groups and 2–bridge knot groups, I*, Lecture Notes in Mathematics 1909, Springer (2007) MR

[2] **F Bonahon**, **J-P Otal**, *Laminations measurées de plissage des variétés hyperboliques de dimension 3*, Ann. of Math. 160 (2004) 1013–1055 MR

[3] **B H Bowditch**, *Markoff triples and quasi-Fuchsian groups*, Proc. London Math. Soc. 77 (1998) 697–736 MR

[4] **R D Canary**, *Pushing the boundary*, from "In the tradition of Ahlfors and Bers, III" (W Abikoff, A Haas, editors), Contemp. Math. 355, Amer. Math. Soc., Providence, RI (2004) 109–121 MR

[5] **Y-E Choi**, **C Series**, *Lengths are coordinates for convex structures*, J. Differential Geom. 73 (2006) 75–117 MR

[6] **M Culler**, *Lifting representations to covering groups*, Adv. in Math. 59 (1986) 64–70 MR

[7] **D B A Epstein**, **A Marden**, *Convex hulls in hyperbolic space, a theorem of Sullivan, and measured pleated surfaces*, from "Analytical and geometric aspects of hyperbolic space" (D B A Epstein, editor), London Math. Soc. Lec. Note Ser. 111, Cambridge Univ. Press (1987) 113–253 MR

[8] **W Fenchel**, *Elementary geometry in hyperbolic space*, De Gruyter Studies in Mathematics 11, De Gruyter, Berlin (1989) MR

[9] **W M Goldman**, *The modular group action on real* SL(2)*–characters of a one-holed torus*, Geom. Topol. 7 (2003) 443–486 MR

[10] **W M Goldman**, *Trace coordinates on Fricke spaces of some simple hyperbolic surfaces*, from "Handbook of Teichmüller theory, Vol II" (A Papadopoulos, editor), IRMA Lect. Math. Theor. Phys. 13, Eur. Math. Soc., Zürich (2009) 611–684 MR

[11] **W Goldman**, **G McShane**, **G Stantchev**, **S P Tan**, *Automorphisms of two-generator free groups and spaces of isometric actions on the hyperbolic plane*, preprint (2015) arXiv

[12] **J Hempel**, 3*–Manifolds*, Ann. of Math. Studies 86, Princeton Univ. Press (1976) MR

[13] **C D Hodgson**, **S P Kerckhoff**, *Rigidity of hyperbolic cone-manifolds and hyperbolic Dehn surgery*, J. Differential Geom. 48 (1998) 1–59 MR

[14] **L Keen**, **C Series**, *Pleating coordinates for the Maskit embedding of the Teichmüller space of punctured tori*, Topology 32 (1993) 719–749 MR

[15] **L Keen**, **C Series**, *The Riley slice of Schottky space*, Proc. London Math. Soc. 69 (1994) 72–90 MR

[16] **L Keen**, **C Series**, *Continuity of convex hull boundaries*, Pacific J. Math. 168 (1995) 183–206 MR

[17] **L Keen**, **C Series**, *How to bend pairs of punctured tori*, from "Lipa's legacy" (J Dodziuk, L Keen, editors), Contemp. Math. 211, Amer. Math. Soc., Providence, RI (1997) 359–387 MR

[18] **L Keen**, **C Series**, *Pleating invariants for punctured torus groups*, Topology 43 (2004) 447–491 MR

[19] **Y Komori**, **C Series**, *The Riley slice revisited*, from "The Epstein birthday schrift" (I Rivin, C Rourke, C Series, editors), Geom. Topol. Monogr. 1, Geom. Topol. Publ., Coventry (1998) 303–316 MR

[20] **I Kra**, *On lifting Kleinian groups to* $\mathrm{SL}(2,\mathbf{C})$, from "Differential geometry and complex analysis" (I Chavel, H M Farkas, editors), Springer (1985) 181–193 MR

[21] **F Luo**, *Simple loops on surfaces and their intersection numbers*, Math. Res. Lett. 5 (1998) 47–56 MR

[22] **S Maloni**, **F Palesi**, **S P Tan**, *On the character variety of the four-holed sphere*, Groups Geom. Dyn. 9 (2015) 737–782 MR

[23] **A Marden**, *Hyperbolic manifolds: an introduction in* 2 *and* 3 *dimensions*, 2nd edition, Cambridge Univ. Press (2016)

[24] **B Maskit**, *Kleinian groups*, Grundl. Math. Wissen. 287, Springer (1988) MR

[25] **S P K Ng**, **S P Tan**, *The complement of the Bowditch space in the* $\mathrm{SL}(2,\mathbb{C})$ *character variety*, Osaka J. Math. 44 (2007) 247–254 MR

[26] **J-P Otal**, *Sur le coeur convexe d'une variété hyperbolique de dimension* 3, preprint (1994) http://www.math.univ-toulouse.fr/~otal/

[27] **C Series**, *The geometry of Markoff numbers*, Math. Intelligencer 7 (1985) 20–29 MR

[28] **C Series**, *An extension of Wolpert's derivative formula*, Pacific J. Math. 197 (2001) 223–239 MR

[29] **S P Tan**, **Y L Wong**, **Y Zhang**, *Necessary and sufficient conditions for McShane's identity and variations*, Geom. Dedicata 119 (2006) 199–217 MR

[30] **S P Tan**, **Y L Wong**, **Y Zhang**, *Generalized Markoff maps and McShane's identity*, Adv. Math. 217 (2008) 761–813 MR

[31] **M Wada**, *Software OPTi* http://delta-mat.ist.osaka-u.ac.jp/OPTi/

[32] **M Wada**, *OPTi's algorithm for discreteness determination*, Experiment. Math. 15 (2006) 61–66 MR

Mathematics Institute, University of Warwick
Leeman Building, Coventry, CV4 7AL, United Kingdom

Department of Mathematics, National University of Singapore
Block S17, 10 Lower Kent Ridge Rd., Singapore 119076

Department of Information and Computer Sciences, Nara Women's University
Kitauoyanishi-machi, Nara 630-8506, Japan

c.m.series@warwick.ac.uk, mattansp@nus.edu.sg, yamasita@ics.nara-wu.ac.jp

http://homepages.warwick.ac.uk/~masbb/, http://www.math.nus.edu.sg/~mattansp/, http://vivaldi.ics.nara-wu.ac.jp/~yamasita/

Received: 17 April 2016 Revised: 17 October 2016